FLUIDICS & BIOCOMPLEXITY GROUP

UCL

Integrative Modelling of Brain Transport Phenomena: From Hydrocephalus to Dementia

John Vardakis

Dean Chou

Liwei Guo

Brett Tully

y.ventikos@ucl.ac.uk Yiannis Ventikos

- Physiology, Motivation and Model Specifications
- Modelling Approach
- Applications & Results
- Hybrid Approaches for Brain IT-based Healthcare
- Conclusions & Work in Progress

www.jeffhurtblog.com

BLOOD

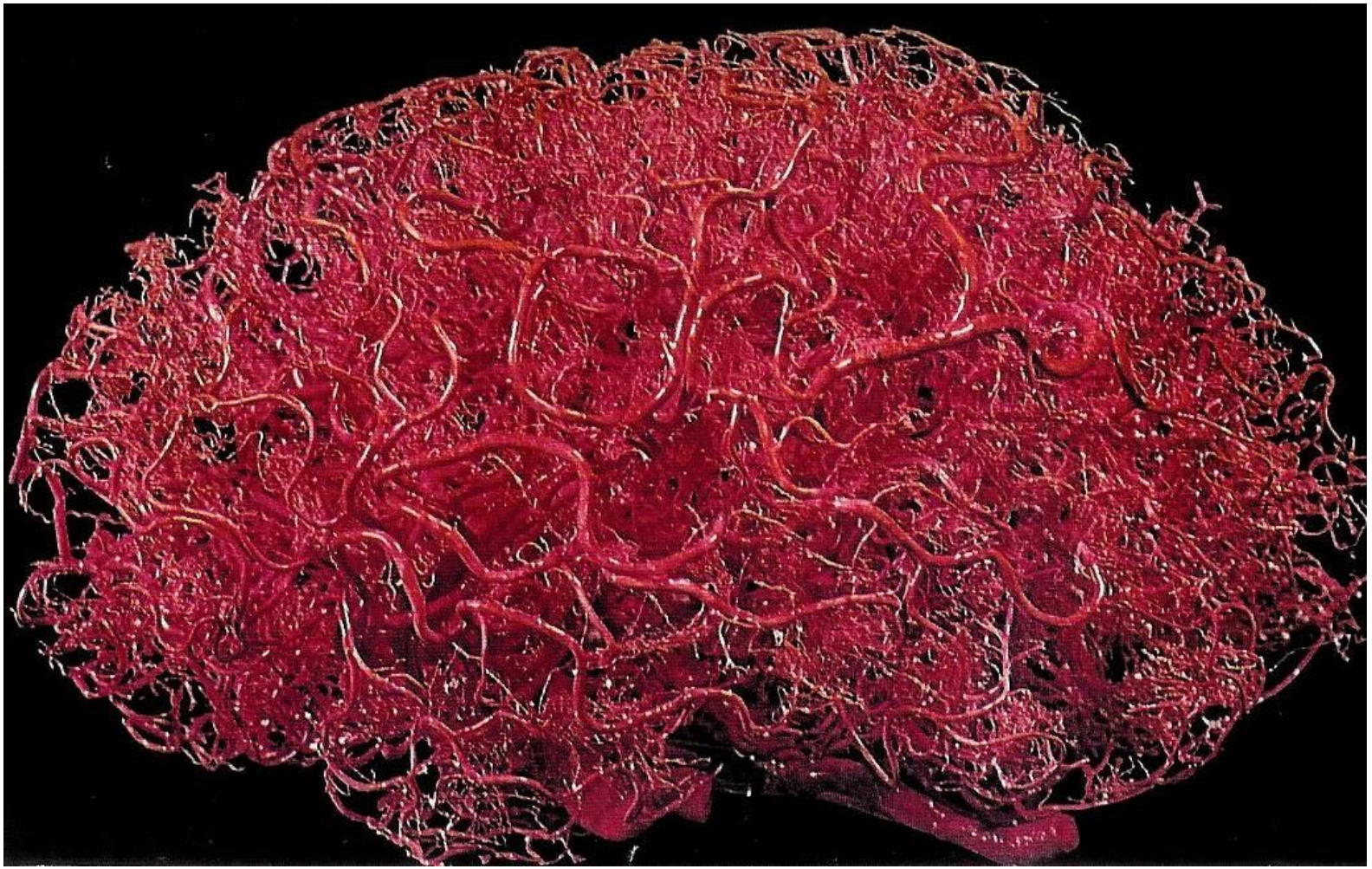

The brain: The most vascularised organ

Hadjistassou et al. Cerebral oxygenation and optimal vascular brain organization.
J. R. Soc. Interface 12: 20150245, 2015

BLOOD

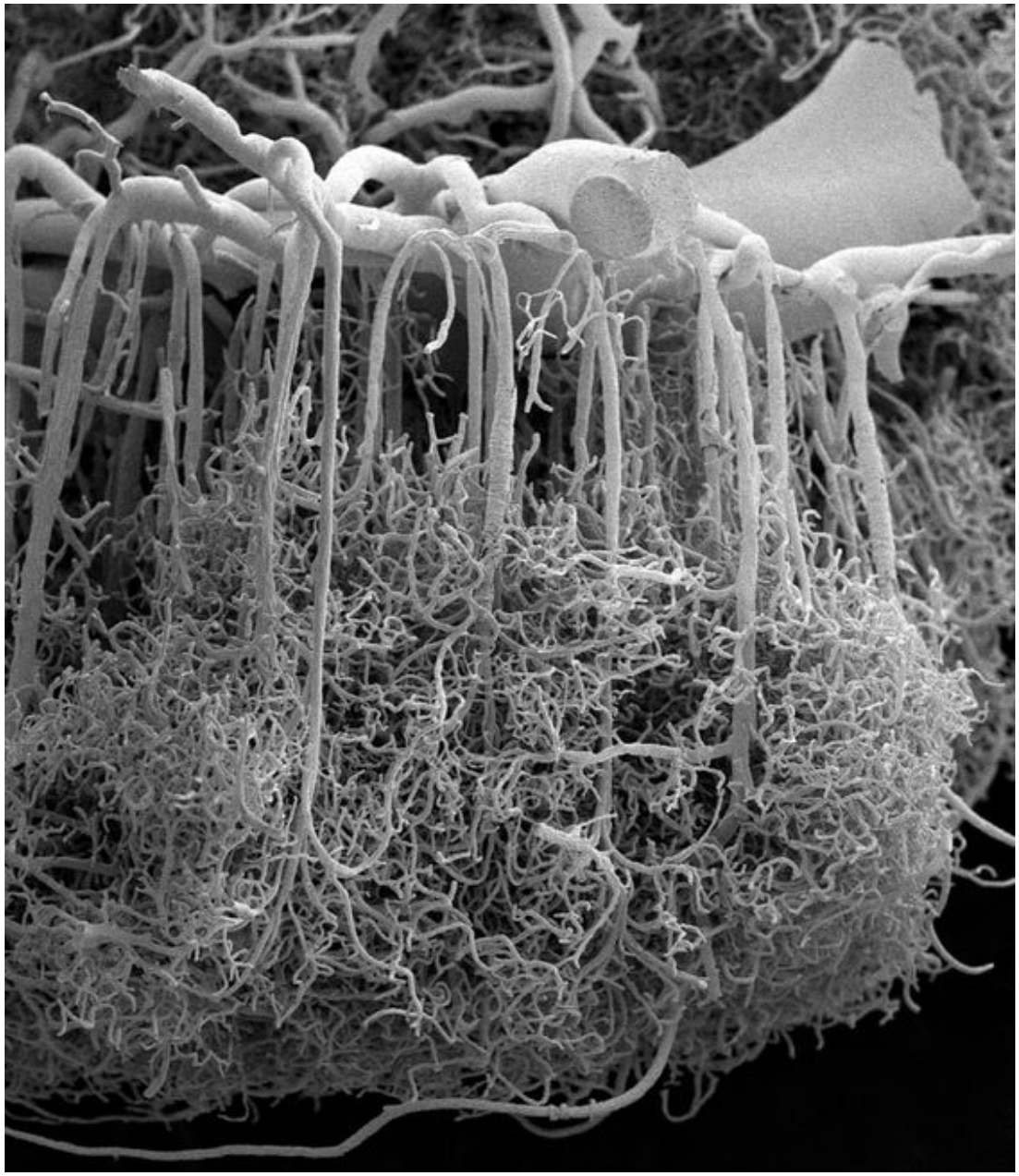

Main Brain Function: Cognition.
Can we couple with biomechanics?

- Haemoglobin: 95%-98% of O_2 carried in blood is chemically bound to Hb.

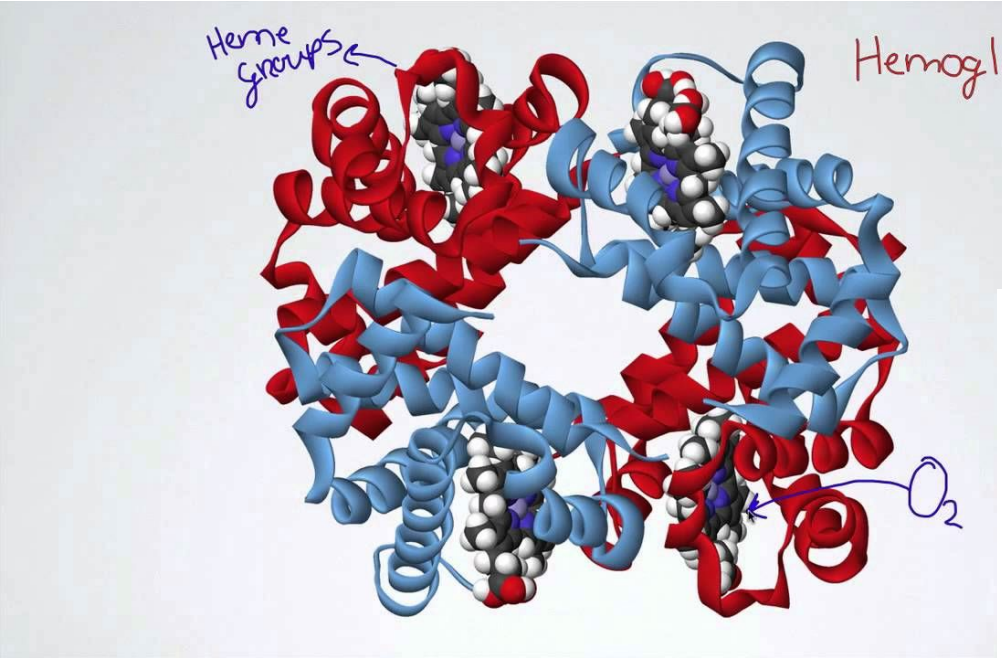

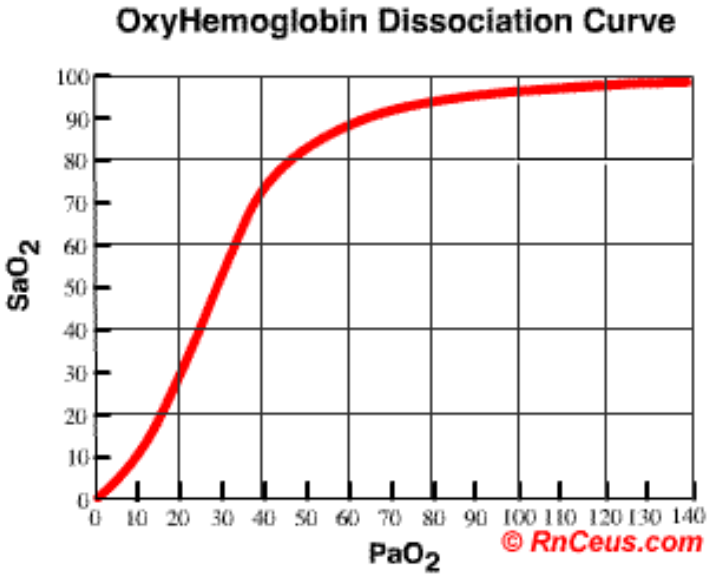

- Oxygenated vs Deoxygenated Haemoglobin: Magnetically different (therefore different signals in MRI).

Main Brain Function: Cognition.
Can we couple with biomechanics?

- Brain has no oxygen reserves and cannot burn glucose anaerobically.
- During activation, (neuronal activity) there is (local) increased metabolic demand.
- This demand is overcompensated by a disproportional increase in local cerebral blood flow (CBF): During activation, the regional cerebral metabolic rate for oxygen (rCMRO2) increases by about 5% but the rCBF increases by almost 30%.
- The mechanism by which the neural system provides feedback to the vascular system is not yet completely understood. The prevailing theory is that the release of glutamate as part of neuron firing affects nearby astrocytes, causing a change in calcium ion concentration. This, in turn, releases nitric oxide at the contact point of astrocytes which vasodilates local arterioles.

Main Brain Function: Cognition.
Can we couple with biomechanics?

- A general capillary-tissue transport model.
- Solve for convection, diffusion and chemical reaction, depending on the region.

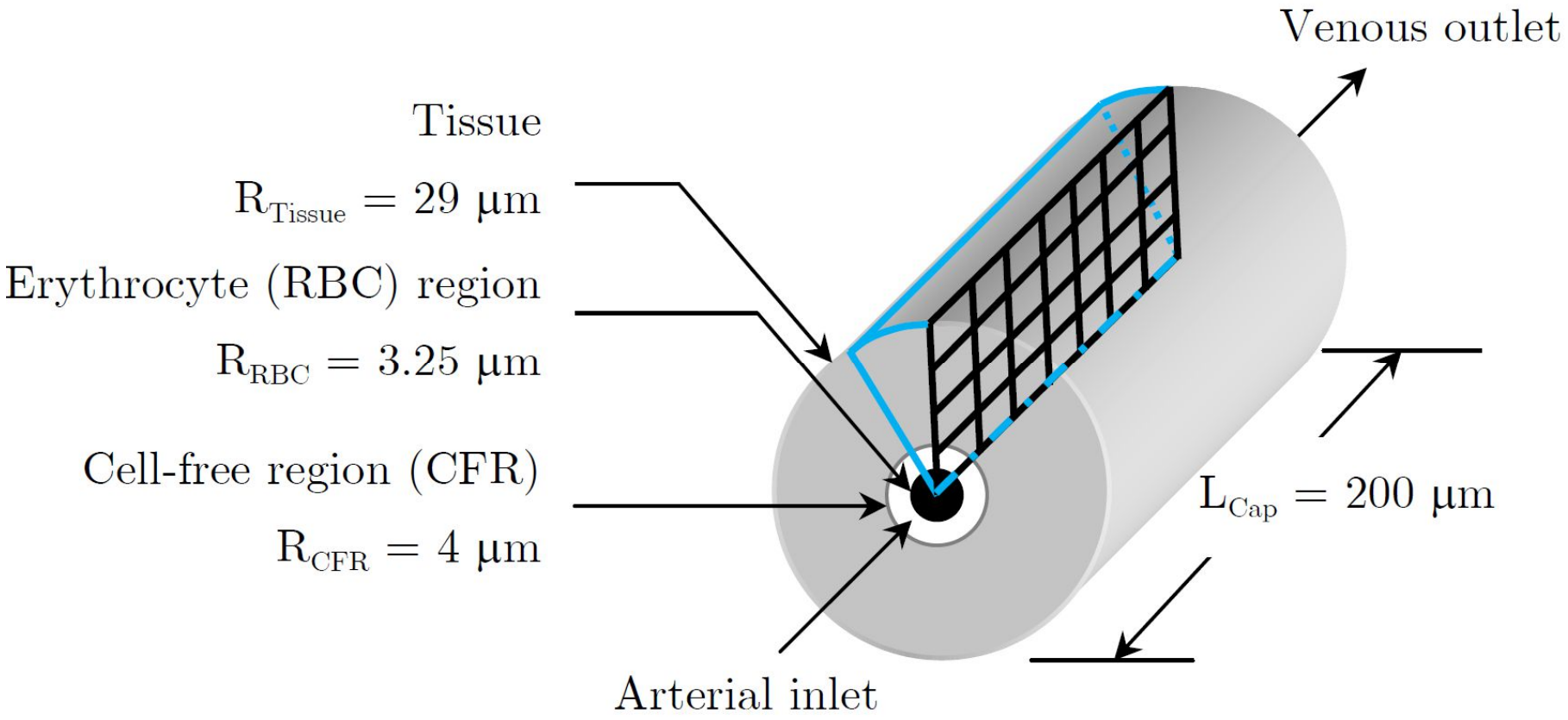

Main Brain Function: Cognition.
Can we couple with biomechanics?

- A general capillary-tissue transport model

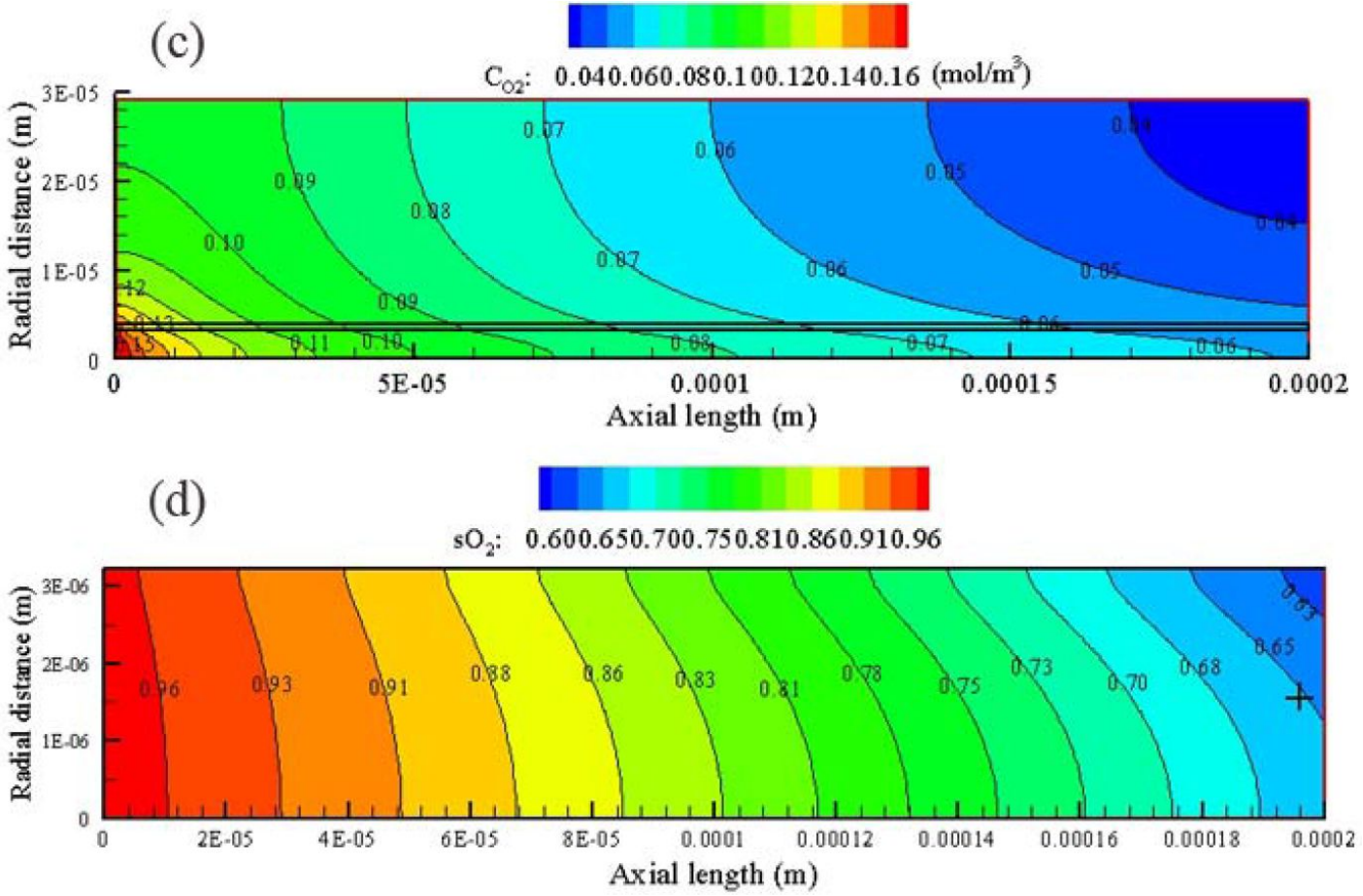

Main Brain Function: Cognition.
Can we couple with biomechanics?

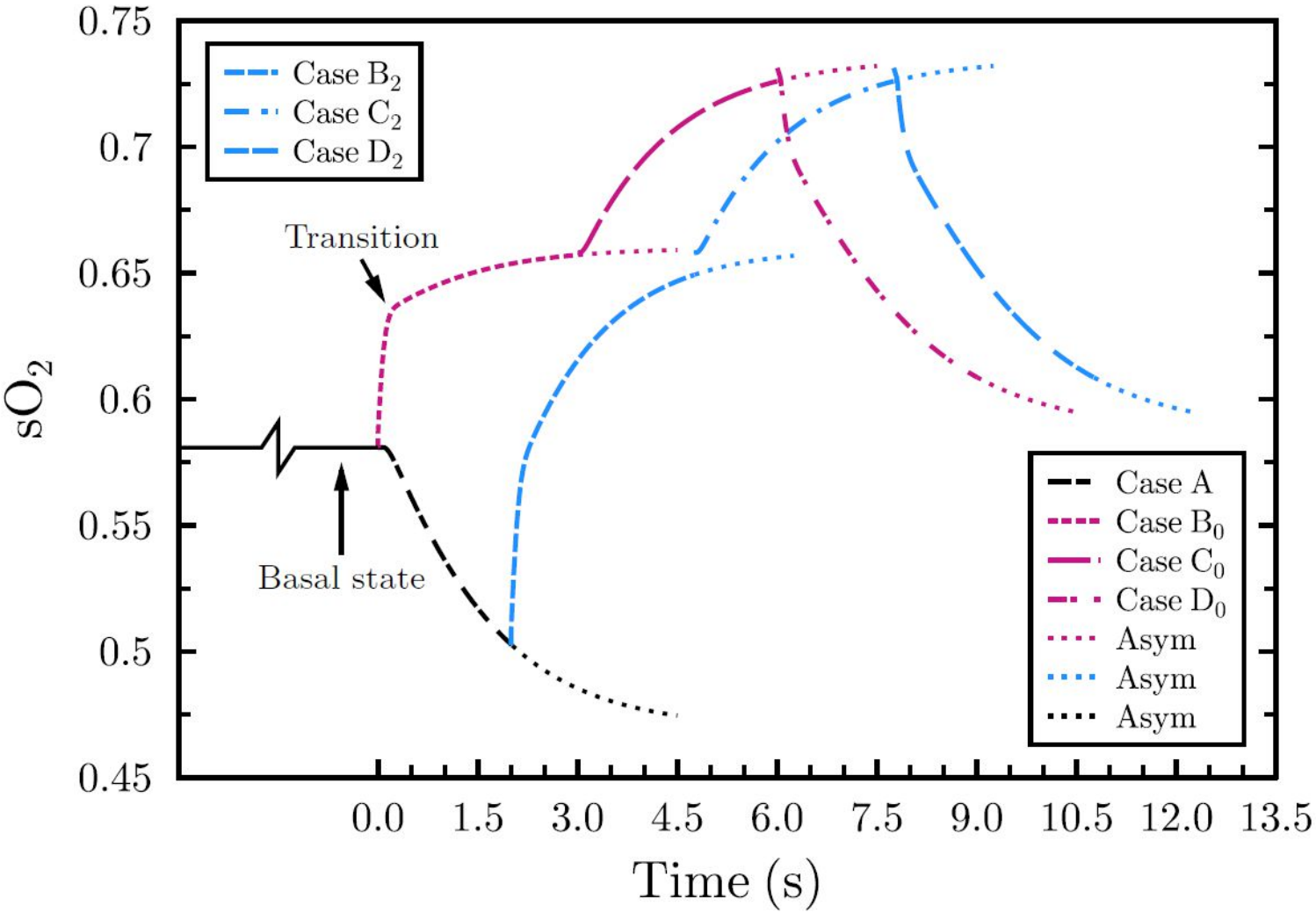

CEREBROSPINAL FLUID (CSF)

- A clear watery fluid
- The brain is “bathed” and “floats” in CSF
- Shock absorber
- According to the classical hypothesis, CSF is produced in the cerebral ventricles which are situated deep within the brain parenchyma
- CSF is absorbed primarily at the skull (classical hypothesis)
- CSF is necessary to maintain “constant ICP”
- Around 600-650 *ml* is produced every day with a volume turnover of ~ four.

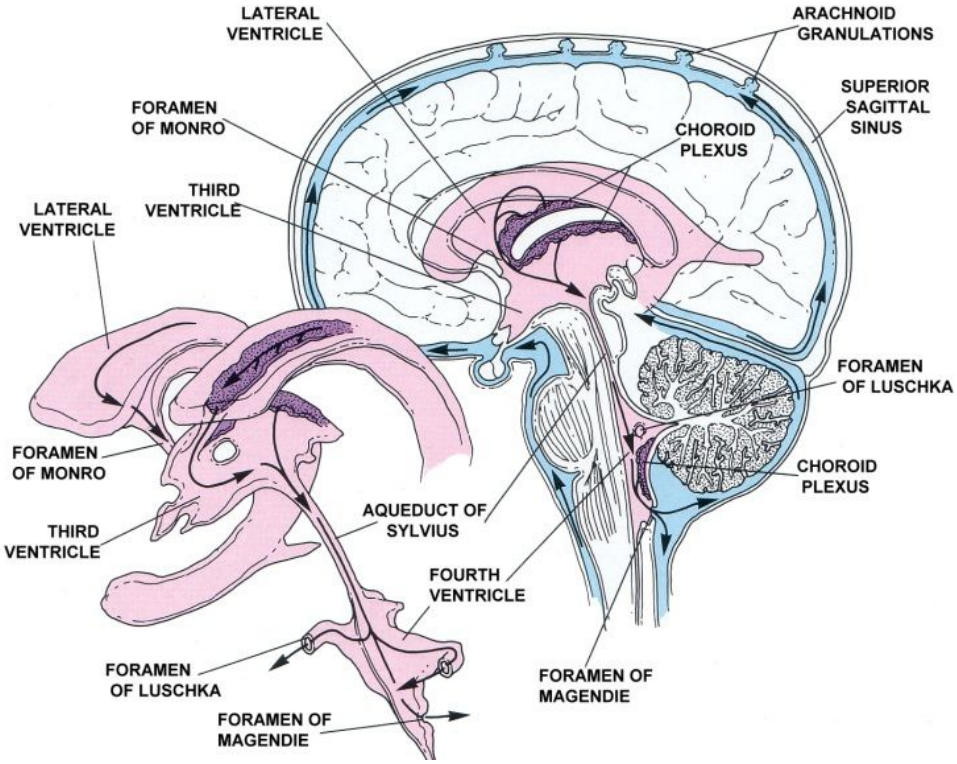

CSF movement

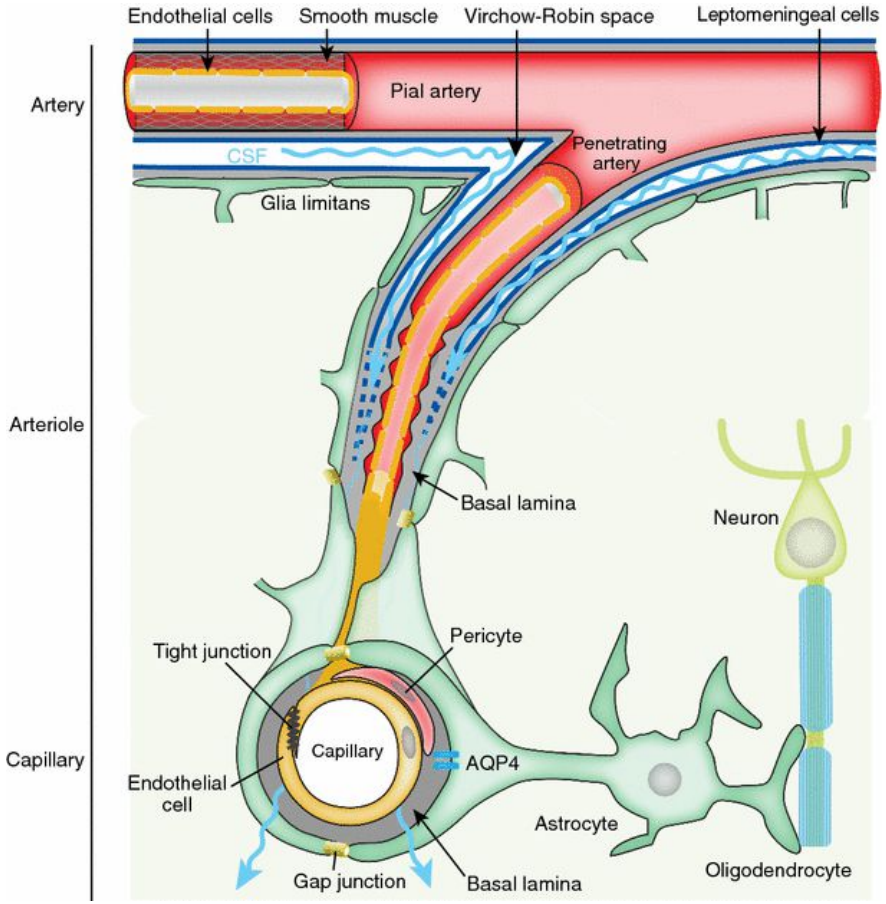

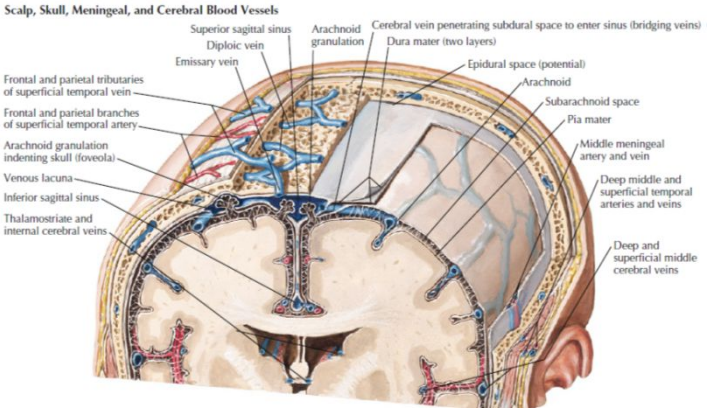

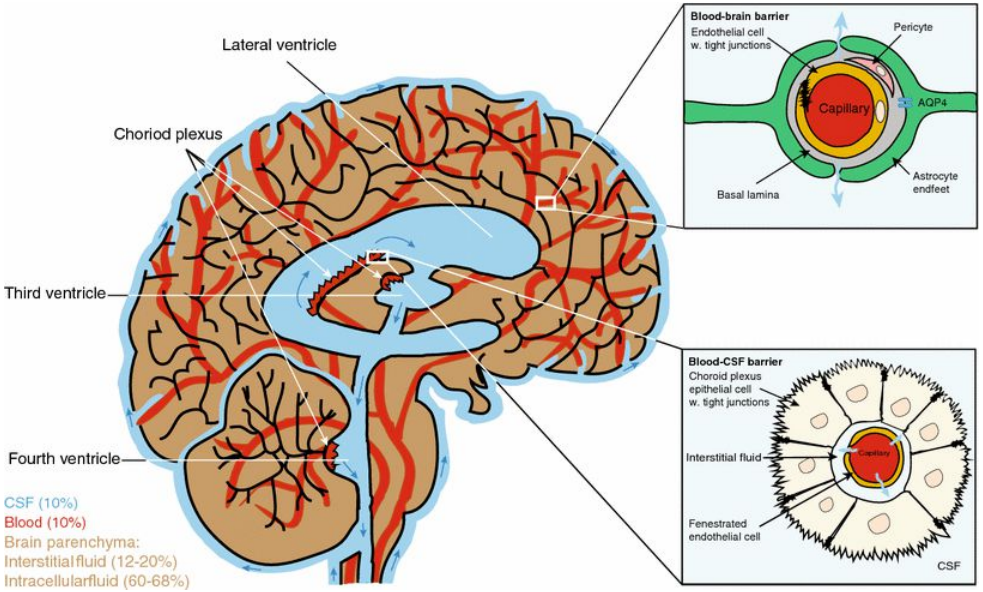

Jessen et al., Neurochem Res (2015)

Aquaporins (Astrocytic AQP4)

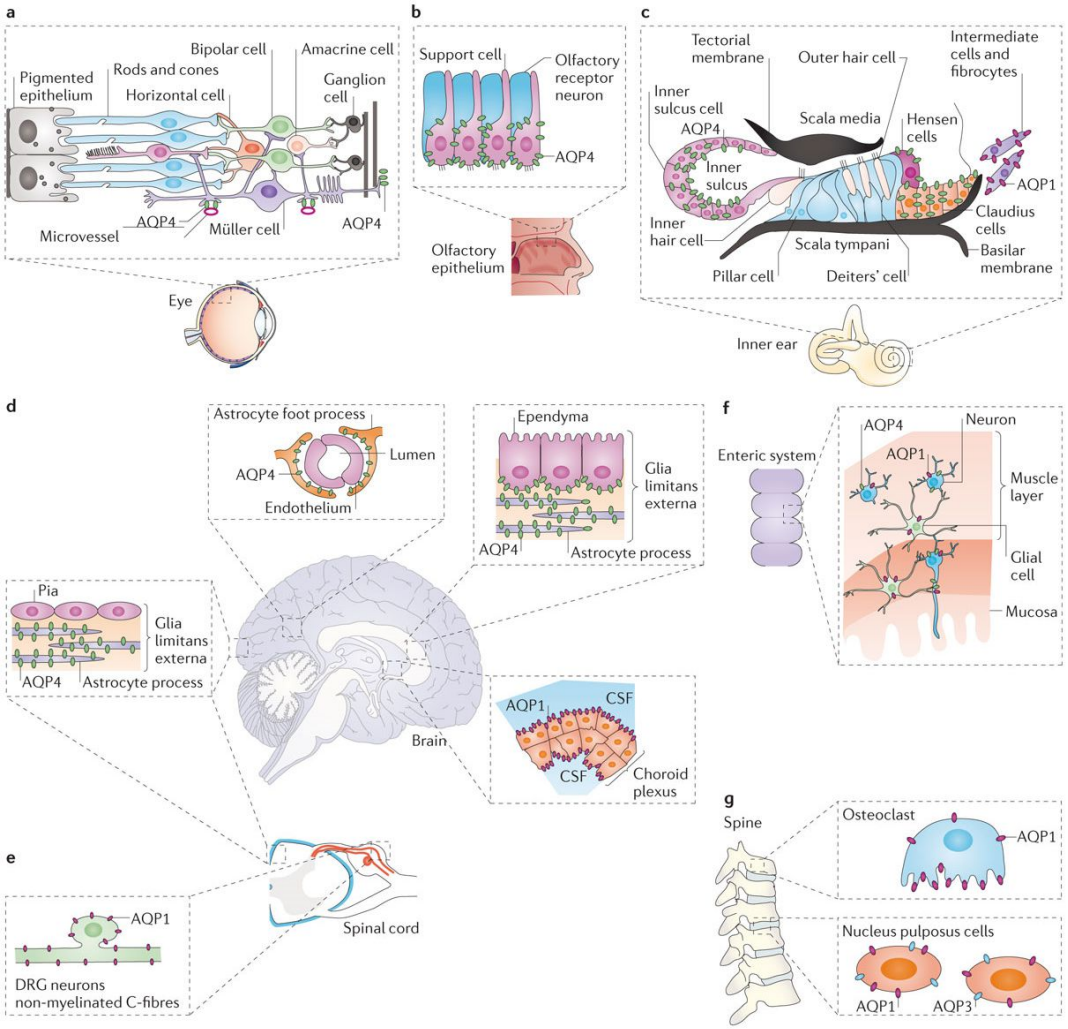

Papadopoulos & Verkman.(2013)

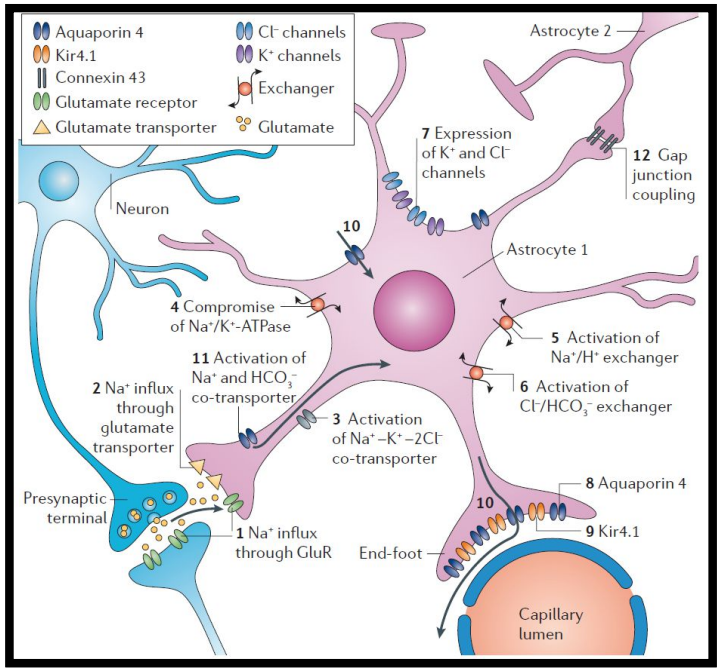

Seifert et al., Nat. Rev. Neuro. (2006)

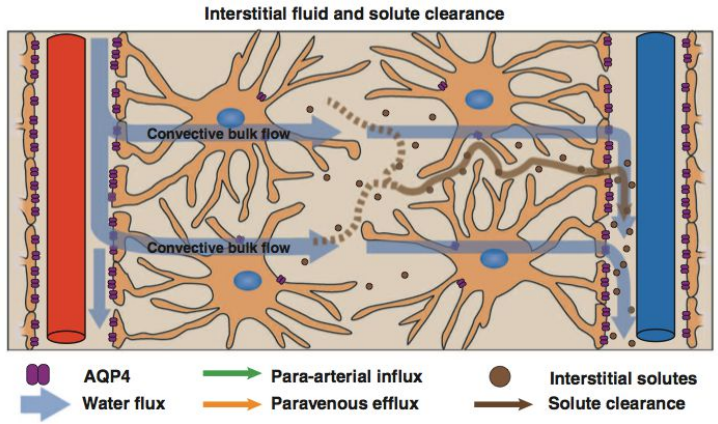

Iliff et al., Sci. Transl. Med. (2012)

Aquaporins (Astrocytic AQP4)

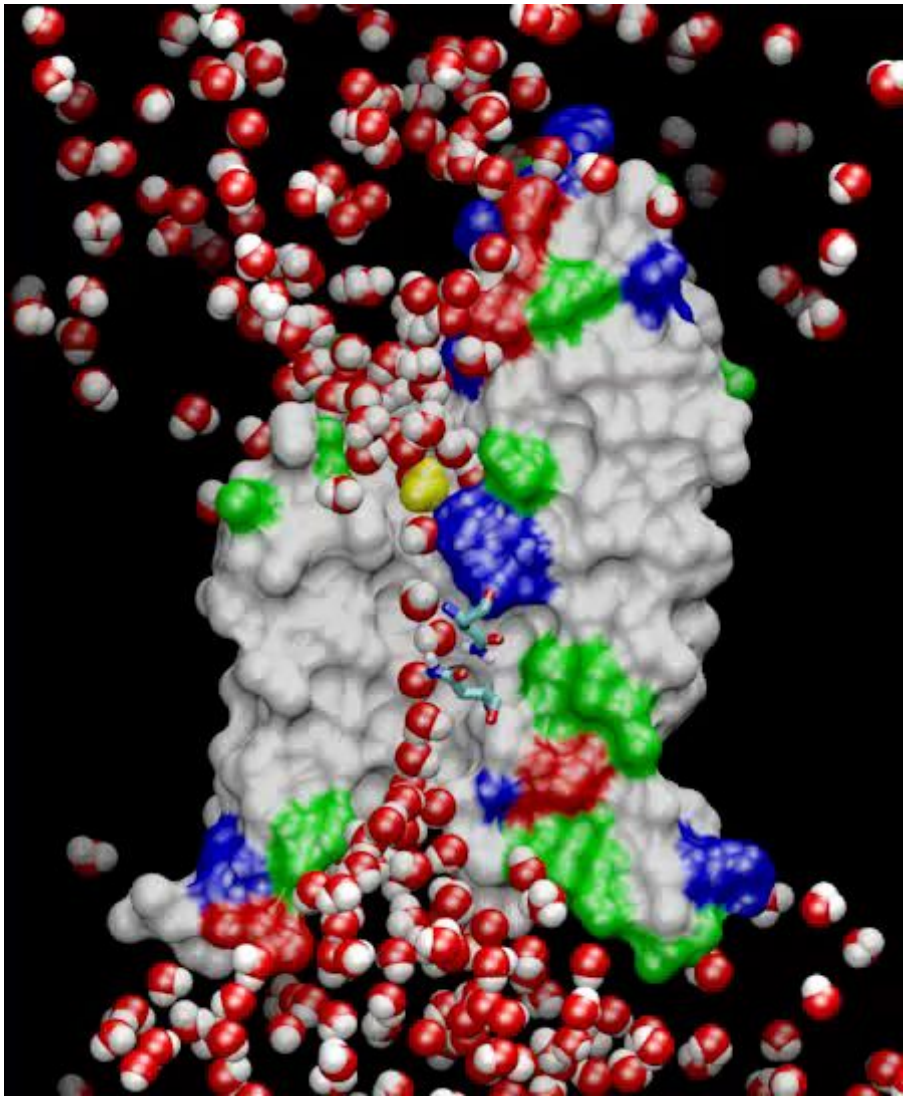

Theoretical and Computational Biophysics Group , University of Illinois at Urbana-Champaign

http://www.ks.uiuc.edu/Research/aquaporins/

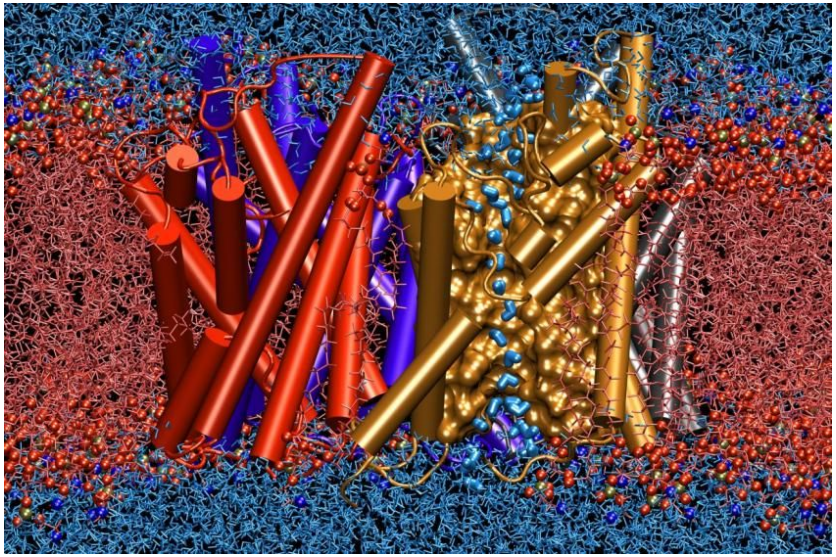

Scales

The inherent multiscalarity of the cerebral water flow environment:

- from ventricles and aqueducts (-A- cm-mm)
- to the subarachnoid space (-B- mm-µm)
- to glial end-feet and capillaries(-C- µm)
- to channels and tight junctions (-D- nm or below)

If all channels and tight junctions push water unidirectionally, the flux is much larger than the pulsatile largest scale flux…

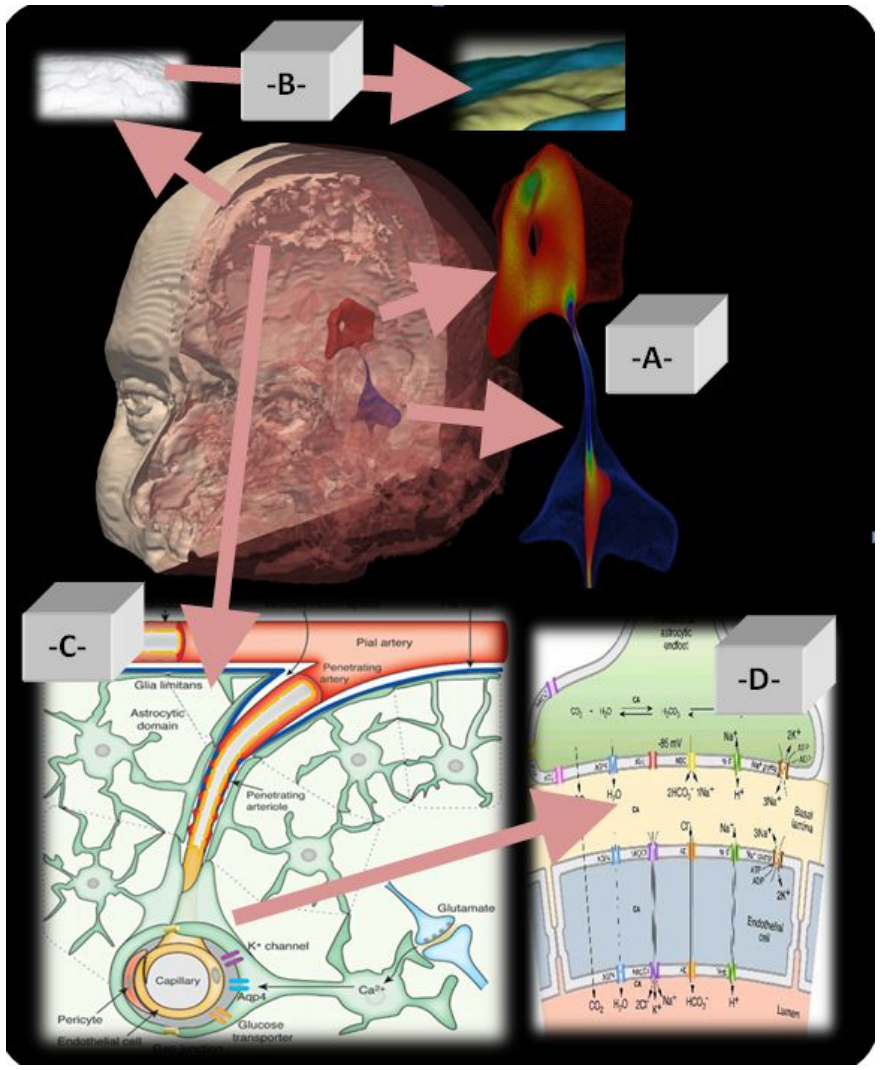

So, there is blood and CSF.

CSF was universally acknowledged and started being characterised only in the 70s. It is worth remembering always that it is a blood filtrate.

Then, recently, two seminal (to be?) papers force us to rethink:

- L. Xie et al., Sleep Drives Metabolite Clearance from the Adult Brain, *Science,* 342(6156), 18 October 2013
  - ***The glymphatic perivascular system***

- A. Louveau et al, Structural and functional features of central nervous system lymphatic vessels, *Nature,* 16;523(7560), 2015
  - ***A proper lymphatic system in the head***

Motivation: Diseases - Treatments

- Hydrocephalus
- Chiari Malformations
- Cerebral Oedema
- Stroke
- Vasospasms
- Traumatic Brain Impact Injury
- Dementia (ALZ, Vascular, FTD etc)

- Early and Differential Dementia Diagnosis
- Shunting
- Third/Fourth Ventriculostomy

FLUIDICS & BIOCOMPLEXITY GROUP

UCL

Shift in attention?

REVIEWS

Clearance systems in the brain—implications for Alzheimer disease

Jenna M. Tarasoff-Conway, Roxana O. Carare, Ricardo S. Osorio, Lidia Glodzik, Tracy Butler, Els Fieremans, Leon Axel, Henry Rusinek, Charles Nicholson, Berislav V. Zlokovic, Blas Frangione, Kaj Blennow, Joël Ménard, Henrik Zetterberg, Thomas Wisniewski and Mony J. de Leon

Abstract | Accumulation of toxic protein aggregates—amyloid-β (Aβ) plaques and hyperphosphorylated tau tangles—is the pathological hallmark of Alzheimer disease (AD). Aβ accumulation has been hypothesized to result from an imbalance between Aβ production and clearance; indeed, Aβ clearance seems to be impaired in both early and late forms of AD. To develop efficient strategies to slow down or halt AD, it is critical to understand how Aβ is cleared from the brain. Extracellular Aβ deposits can be removed from the brain by various clearance systems, most importantly, transport across the blood–brain barrier. Findings from the past few years suggest that astroglial-mediated interstitial fluid (ISF) bulk flow, known as the glymphatic system, might contribute to a larger portion of extracellular Aβ (eAβ) clearance than previously thought. The meningeal lymphatic vessels, discovered in 2015, might provide another clearance route. Because these clearance systems act together to drive eAβ from the brain, any alteration to their function could contribute to AD. An understanding of Aβ clearance might provide strategies to reduce excess Aβ deposits and delay, or even prevent, disease onset. In this Review, we describe the clearance systems of the brain as they relate to proteins implicated in AD pathology, with the main focus on Aβ.

Tarasoff-Conway, J. M. *et al. Nat. Rev. Neurol.* advance online publication 21 July 2015; doi:10.1038/nrneurol.2015.119

New York University School of Medicine, 660 First Avenue, New York, NY 10016, USA (J.M.T.C., E.F., L.A., C.N.). University of Southampton, Faculty of Medicine, Institute for Life Sciences, Southampton General Hospital, Southampton Hampshire, SO16 6YD, UK (R.O.C.). New York University School of Medicine, 145 East 32nd Street, New York, NY 10016, USA (R.S.O., L.G., T.B., H.R., B.F., T.W., M.J.d.L.). Zilkha Neurogenetic Institute at Keck School of Medicine of University of Southern California, 1501 San Pablo Street Los Angeles, CA 90089, USA (B.V.Z.). The Sahlgrenska Academy at the University of Gothenburg, S-431 80 Mölndal, Sweden (K.B., H.Z.). Université Paris-Descartes, 12 Rue de l'École de Médecine, 75006 Paris, France (J.M.).

Correspondence to: M.J.d.L. mony.deleon@nyumc.org

Introduction

Alzheimer disease (AD) is the most common type of dementia and comprises early-onset AD (EOAD) and sporadic or late-onset AD (LOAD).[1–3] EOAD affects a minority of AD patients, whereas LOAD afflicts over 95% of patients with AD.[4–6] Both EOAD and LOAD are characterized by excessive accumulation of toxic forms of amyloid-β (Aβ), which has been hypothesized to result from an imbalance between its production and clearance.[7–9] Emerging evidence suggests that Aβ clearance is impaired in both early-onset and late-onset forms of AD.[10,11] Specifically, carriers of EOAD-associated presenilin mutations show both increased Aβ production[10,12] and decreased Aβ clearance,[10] whereas individuals with LOAD exhibit decreased Aβ clearance only.[11]

Failure of Aβ clearance is increasingly recognized in the pathogenesis of AD. It is critical to understand how Aβ is cleared from the brain, and to find new ways of investigating this process in carefully phenotyped patients and healthy controls. Because Aβ deposition can be increased in presymptomatic individuals years or even decades before the hallmark symptoms of AD manifest,[20] an understanding of Aβ clearance might eventually provide strategies to reduce excess Aβ deposits and delay, or even prevent, disease onset.

Competing interests
K.B. and H.Z. are co-founders of Brain Biomarker Solutions. The other authors declare no competing interests.

Soluble Aβ can be removed from the brain by various clearance systems, including enzymatic degradation and cellular uptake, transport across the blood–brain barrier (BBB) and blood–cerebrospinal fluid barrier (BCSFB), interstitial fluid (ISF) bulk flow, and cerebrospinal fluid (CSF) absorption into the circulatory and lymphatic systems.

In the early 2000s, mouse studies demonstrated that the majority (75%) of extracellular Aβ (eAβ) is cleared by the BBB, with only a minority (10%) being cleared by ISF bulk flow.[14,15] However, two-photon imaging studies from the past few years have suggested that ISF bulk flow—facilitated by astroglial aquaporin-4 (AQP4) channels and named the glymphatic (glial + lymphatic) system—contributes to a larger portion of eAβ clearance than previously thought.[16,17] Furthermore, the discovery of meningeal lymphatic vessels suggests yet another potential clearance route.[18] Although the relative contributions of each of these systems to overall clearance are unknown, they act together to drive eAβ from the brain, meaning that alterations in any given system can contribute to the altered pathophysiology and accumulation of lesions in AD.

In this Review, we aim to describe the brain's clearance systems that are related to removal of toxic accumulation of proteins in AD. Here, 'clearance' is defined broadly as the removal of any substance, such as Aβ, from the brain. We focus on Aβ, given its ability to form aggregates

The Journal of Neuroscience, February 11, 2015 • 35(6):2485–2491 • 2485

Neurobiology of Disease

Inspiration Is the Major Regulator of Human CSF Flow

Steffi Dreha-Kulaczewski,[1] Arun A. Joseph,[2,3] Klaus-Dietmar Merboldt,[2] Hans-Christoph Ludwig,[4] Jutta Gärtner,[1] and Jens Frahm[2,3]

[1]Department of Pediatrics and Adolescent Medicine, Division of Pediatric Neurology, University Medical Center Göttingen, 37075 Göttingen, Germany, [2]Biomedizinische NMR Forschungs GmbH am Max-Planck-Institut für biophysikalische Chemie, 37077 Göttingen, Germany, [3]DZHK (German Center for Cardiovascular Research), 37075 Göttingen, Germany, and [4]Department of Neurosurgery, Division of Pediatric Neurosurgery, University Medical Center Göttingen, 37075 Göttingen, Germany

The mechanisms behind CSF flow in humans are still not fully known. CSF circulates from its primary production sites at the choroid plexus through the brain ventricles to reach the outer surface of the brain in the subarachnoid spaces from where it drains into venous bloodstream and cervical lymphatics. According to a recent concept of brain fluid transport, established in rodents, CSF from the brain surface also enters the brain tissue along para-arterial routes and exits through paravenous spaces again into subarachnoid compartments. This unidirectional flow is mainly driven by arterial pulsation. To investigate how CSF flow is regulated in humans, we applied a novel real-time magnetic resonance imaging technique at high spatial (0.75 mm) and temporal (50 ms) resolution in healthy human subjects. We observed significant CSF flow exclusively with inspiration. In particular, during forced breathing, high CSF flow was elicited during every inspiration, whereas breath holding suppressed it. Only a minor flow component could be ascribed to cardiac pulsation. The present results unambiguously identify inspiration as the most important driving force for CSF flow in humans. Inspiratory thoracic pressure reduction is expected to directly modulate the hydrostatic pressure conditions for the low-resistance paravenous, venous, and lymphatic clearance routes of CSF. Furthermore, the experimental approach opens new clinical opportunities to study the pathophysiology of various forms of hydrocephalus and to design therapeutic strategies in relation to CSF flow alterations.

Key words: **CSF flow; driving force; inspiration; real-time magnetic resonance imaging; respiratory regulation**

Introduction

Although the use of magnetic resonance imaging (MRI) has increased our understanding of human CSF dynamics, the main mechanisms driving CSF flow are still unknown. Brain CSF is contained within subarachnoid spaces and the ventricular system, which is formed by four interconnected cavities (two lateral ventricles, third and fourth ventricles). It circulates from its production site mainly in the choroid plexus of the lateral ventricles through the ventricular system until it reaches the exterior surfaces of brain and spinal cord in the subarachnoid spaces. Over the past decades, several studies used velocity-encoded phase-contrast MRI techniques with cardiac gating to determine quantitative parameters of this flow, such as velocities and stroke volumes. Most reports focus on the pulsatile nature of the CSF flux, which appears to be craniocaudally oriented during cardiac systole and in the reverse direction during diastole (Enzmann and Pelc, 1991; Nitz et al., 1992; Schroth and Klose, 1992a; Greitz et al., 1993). Changes in blood volume in the intracranial arteries, its distribution into capillaries, and the resulting oscillations of brain parenchyma have been presumed as main initiating factors of CSF pulsations (Henry-Feugeas et al., 2000; Wåhlin et al., 2012). The inward expansion of brain tissue is considered to produce aqueductal flow (Greitz et al., 1994).

In addition, respiration has been shown to influence CSF dynamics via thoracic pressure changes in previous studies using invasive manometer recordings (Williams, 1981). Only very few MRI studies avoided cardiac gating by one-dimensional imaging (Schroth and Klose, 1992b), dynamic echo-planar imaging (Kao et al., 2008), or pencil-beam imaging (Bhadelia et al., 2013) or used a cardiac-gated, spin-labeling method during 6 s periods of static breathing conditions (Yamada et al., 2013) to confirm a contribution of respiratory rhythms. However, the majority of MRI studies applied phase-contrast flow MRI sequences with synchronization to the electrocardiogram and therefore confined the observation of CSF dynamics to periodic processes in the range of heart rates.

Recent studies in rodents by Illiff et al. (2012, 2013) have conceptualized a paravascular pathway system for brain fluids (Strittmatter, 2013; Xie et al., 2013) where the pulsation of penetrating cortical arteries drives CSF from the brain surface along para-arterial routes into the tissue (Iliff et al., 2013) and through paravenous routes out into the venous bloodstream, cervical lymphatics, or CSF spaces (Sakka et al., 2011).

Received Aug. 5, 2014; revised Nov. 19, 2014; accepted Dec. 8, 2014.
Author contributions: S.D.-K., H.-C.L., J.G., and J.F. designed research; S.D.-K., A.A.J., K.-D.M., and J.F. performed research; S.D.-K., A.A.J., K.-D.M., and J.F. analyzed data; S.D.-K., J.G., and J.F. wrote the paper.
This work was supported by the Dorothea Schloezer Program of the Georg August University, Göttingen, Germany (S.D.-K.).
The authors declare no competing financial interests.
Correspondence should be addressed to Steffi Dreha-Kulaczewski, Department of Pediatrics and Adolescent Medicine, Division of Pediatric Neurology, University Medical Center Göttingen, Robert-Koch-Str. 40, 37075 Göttingen, Germany. E-mail: sdreha@gwdg.de.
DOI:10.1523/JNEUROSCI.3246-14.2015
 0270-6474/15/352485-07$15.00/0

Dementia

- Alzheimer's, vascular, frontotemporal, etc.
- Overall healthcare cost $1T (or 1% of WGDP)
- Many promising approaches (for diagnosis and treatment) but opinion-makers insist we are decades from "treatment"
- Our understanding of dementia causes has been changing

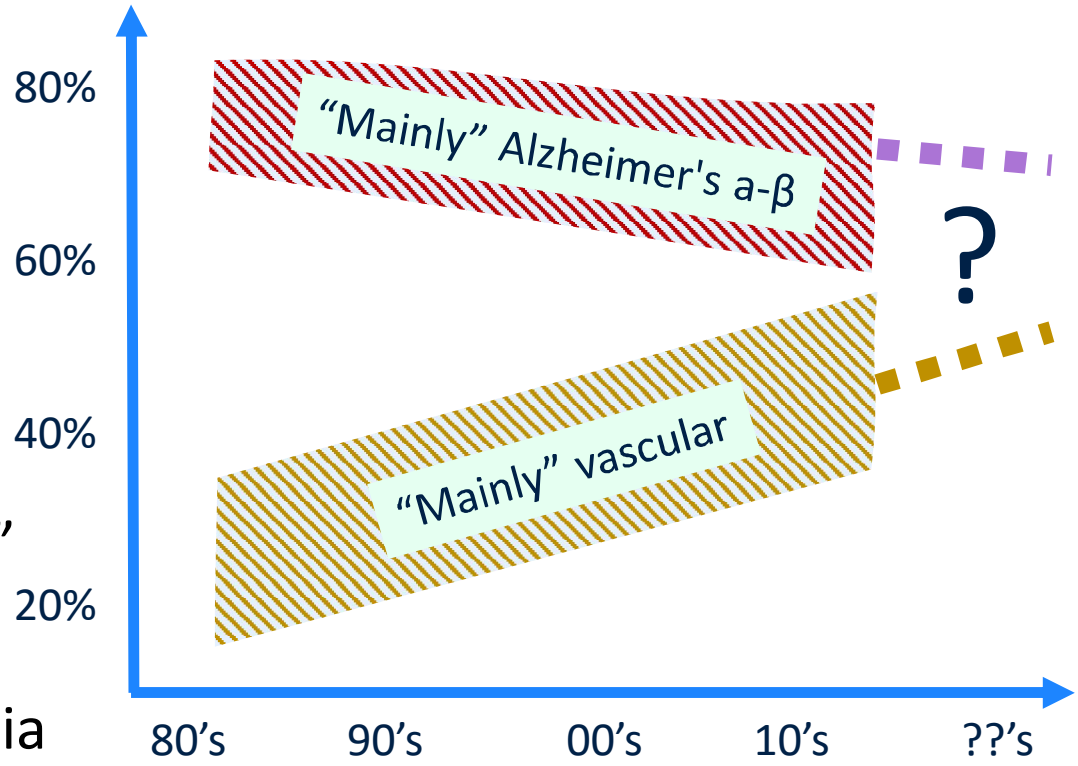

IT-based approaches in Dementia Healthcare & the VPHDARE@IT Project

- The “cognitive vs first principles” impossibility (for the time being!)
- Bring together the best of mechanistic and phenomenological modelling
- Approach the challenges of differential diagnosis and early diagnosis **both** from the top (cognitive impairment assessment) and the bottom (first principles mechanistic approach)

IT-based approaches in Dementia Healthcare & the VPHDARE@IT Project

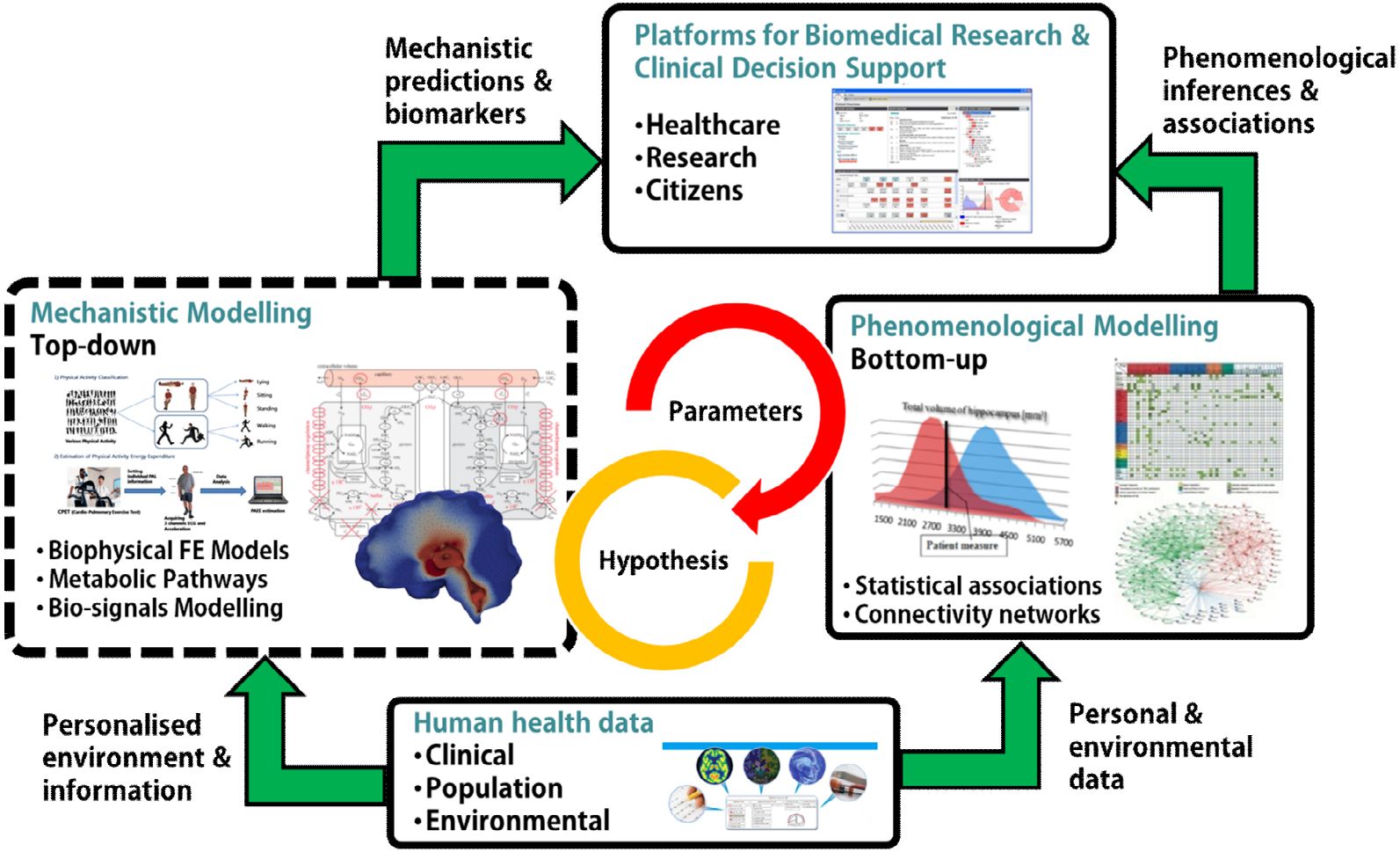

Hydrocephalus

1. Disturbance of formation, flow, or absorption of CSF that leads to an increase in volume occupied by this fluid in the CNS
2. Obvious case for investigation due to its intriguing yet easily observable symptoms
3. Treatment methods display unacceptably high failure rates.

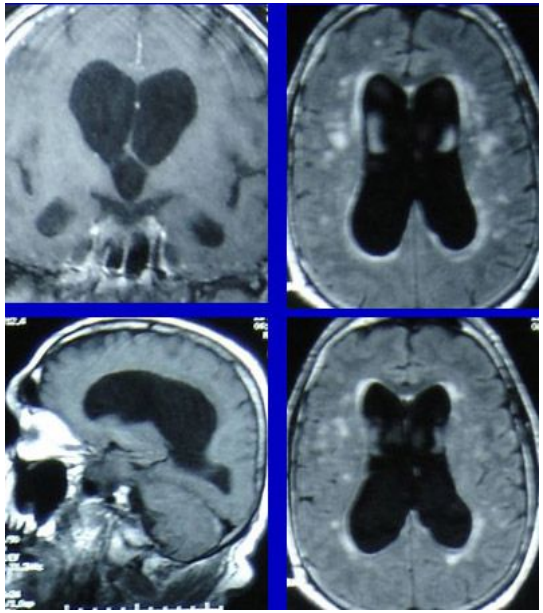

Nevada Imaging Centre

- Acute HCP
- Chronic HCP
- Normal Pressure HCP (NPH)

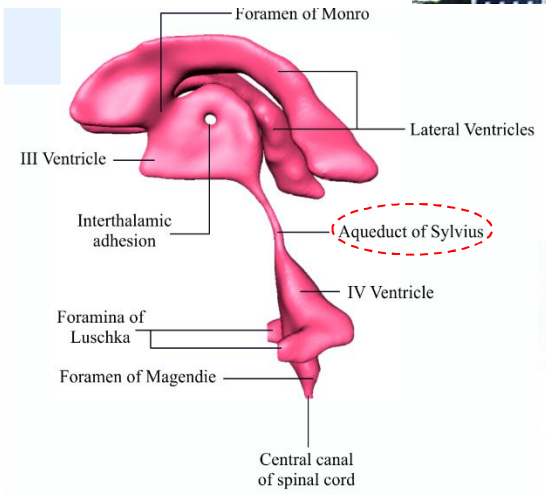

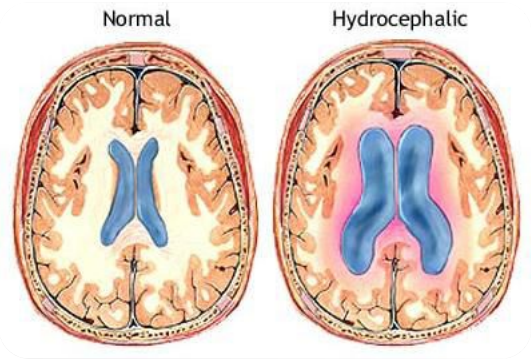

Types of Hydrocephalus

Acute HCP → Caused by intra-ventricular obstruction of CSF pathways - over a period of days

Chronic HCP → A form of HCP with prolonged time scales allowing for its progress

Normal Pressure HCP (NPH) → Rarely occurs in patients below 60. Hakim's triad of symptoms.

Treatments

• Shunting

- Excess CSF to drains to another part of the body
- Consists of two catheters and a one - way valve
- Valve regulated

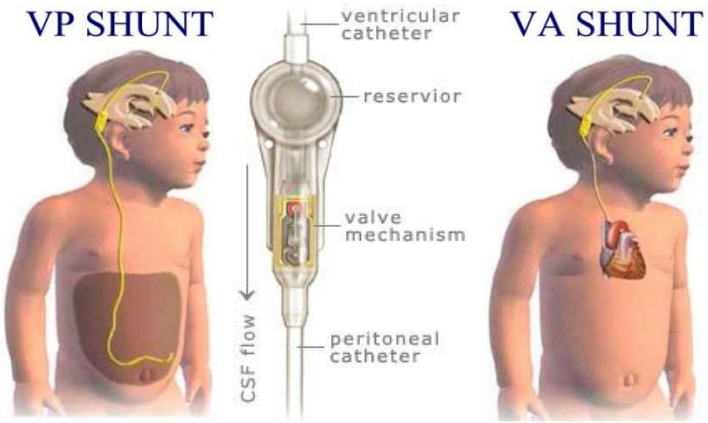

ETV

- Many recommend that ETV be suggested as a first-line treatment to all patients that require management of HCP
- When compared to shunts, ETV also lacks problems in the domains of disconnection, occlusion, high infection rate, overdrainage and valve dysfunction

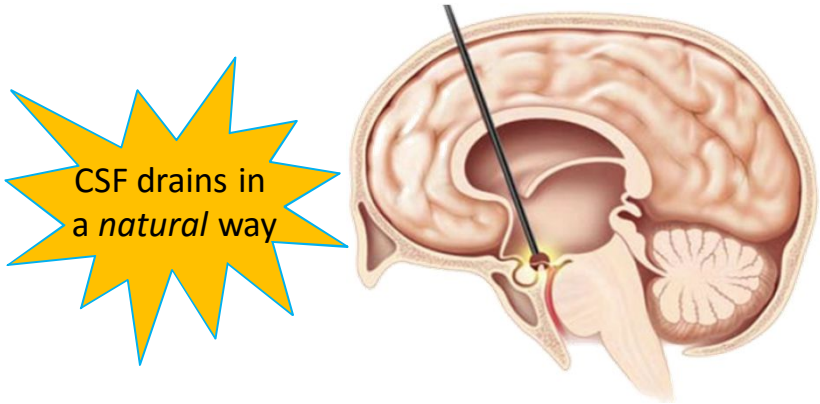

Treatments

In the United States (year 2000), the number of new shunt implantations performed was almost exactly the same as the number of revisions (42.8% vs 43.4%) (Patwardhan & Nanda, 2005).

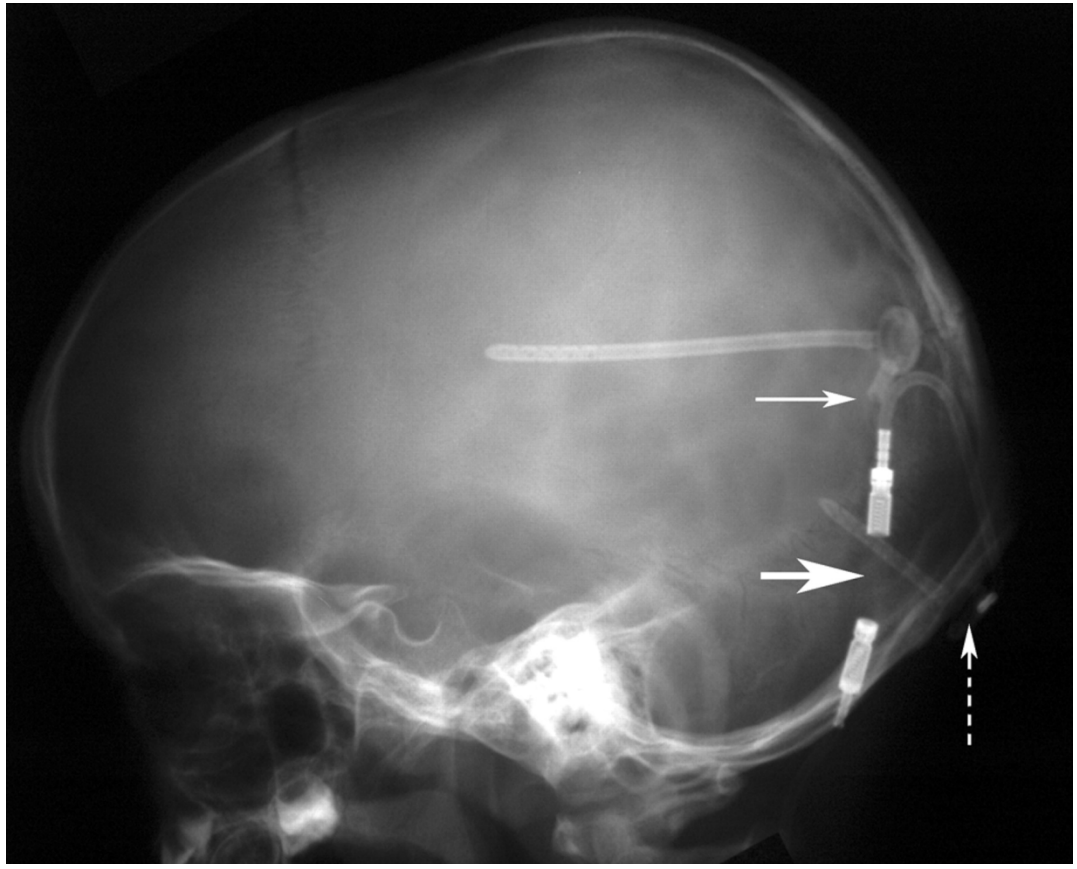

T.S. Satoa, et al., AJNR, 30:635-636, 2009

Treatments

Extremely simple, very cheap

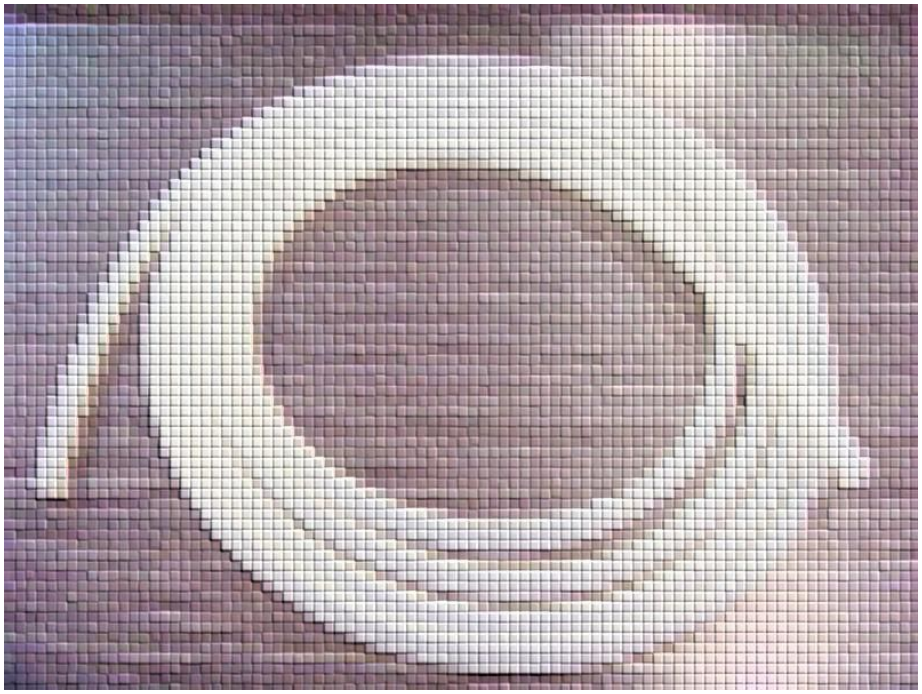

Very sophisticated, rather pricey

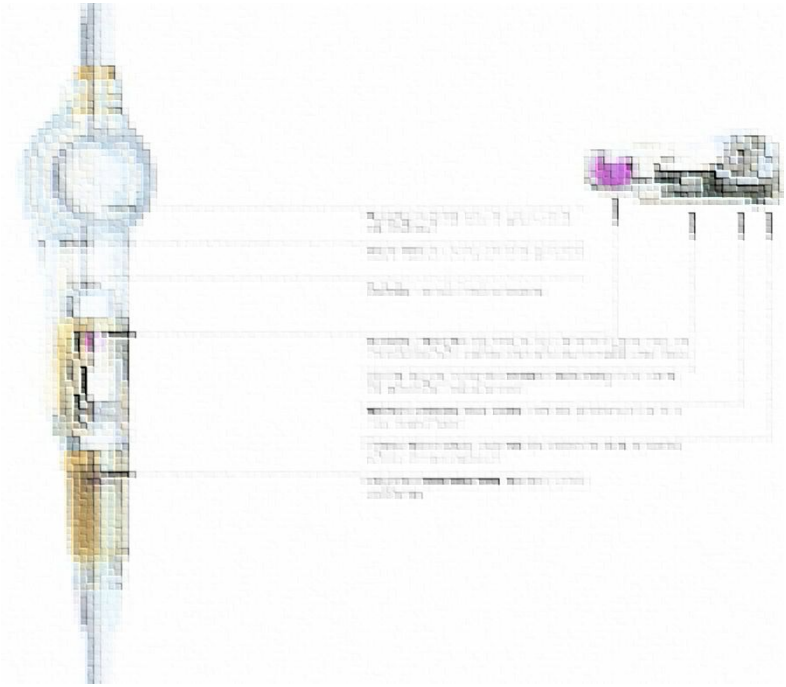

Studies show that very expensive and well-planned treatments (e.g. sophisticated shunts costing almost $1000) can have the same low efficacy with much cheaper ones (often used in developing countries, shunts costing $30-$50)*

*Warf, B. (2005). *J. Neurosurg: Pediatrics*. 4 (102), 358-362

The brain – as a "mechanical" deformable* organ is capable of extreme behaviour!

*Deformation vs Remodelling: Discuss

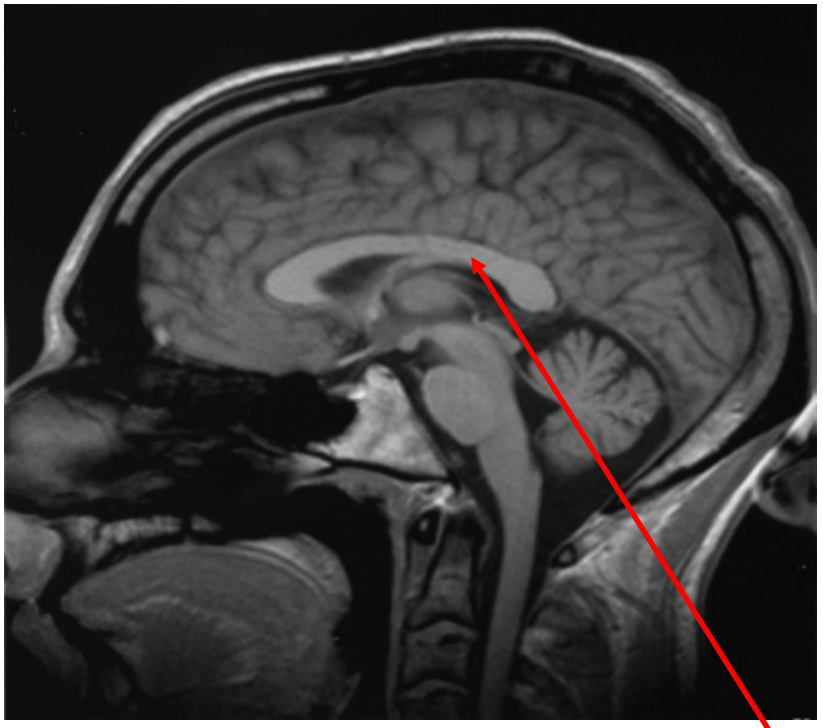

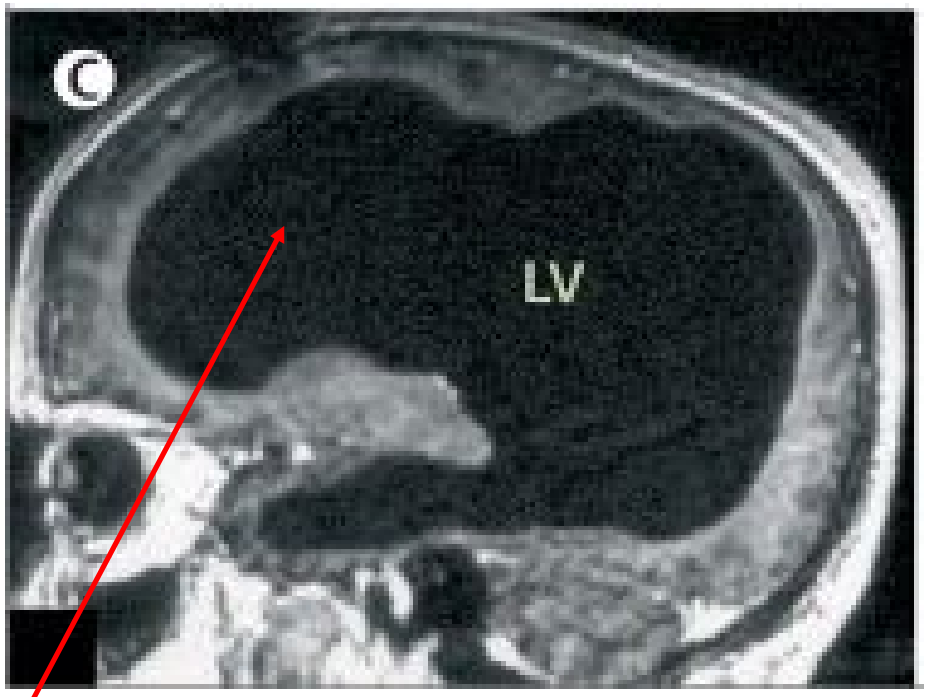

Normal

Lateral ventricles

Certainly not normal

Poroelasticity

Monro-Kellie doctrine:

- Skull is rigid = cranial volume is constant
- Blood enters the brain = something has to give
- CSF is “squeezed” out as a result

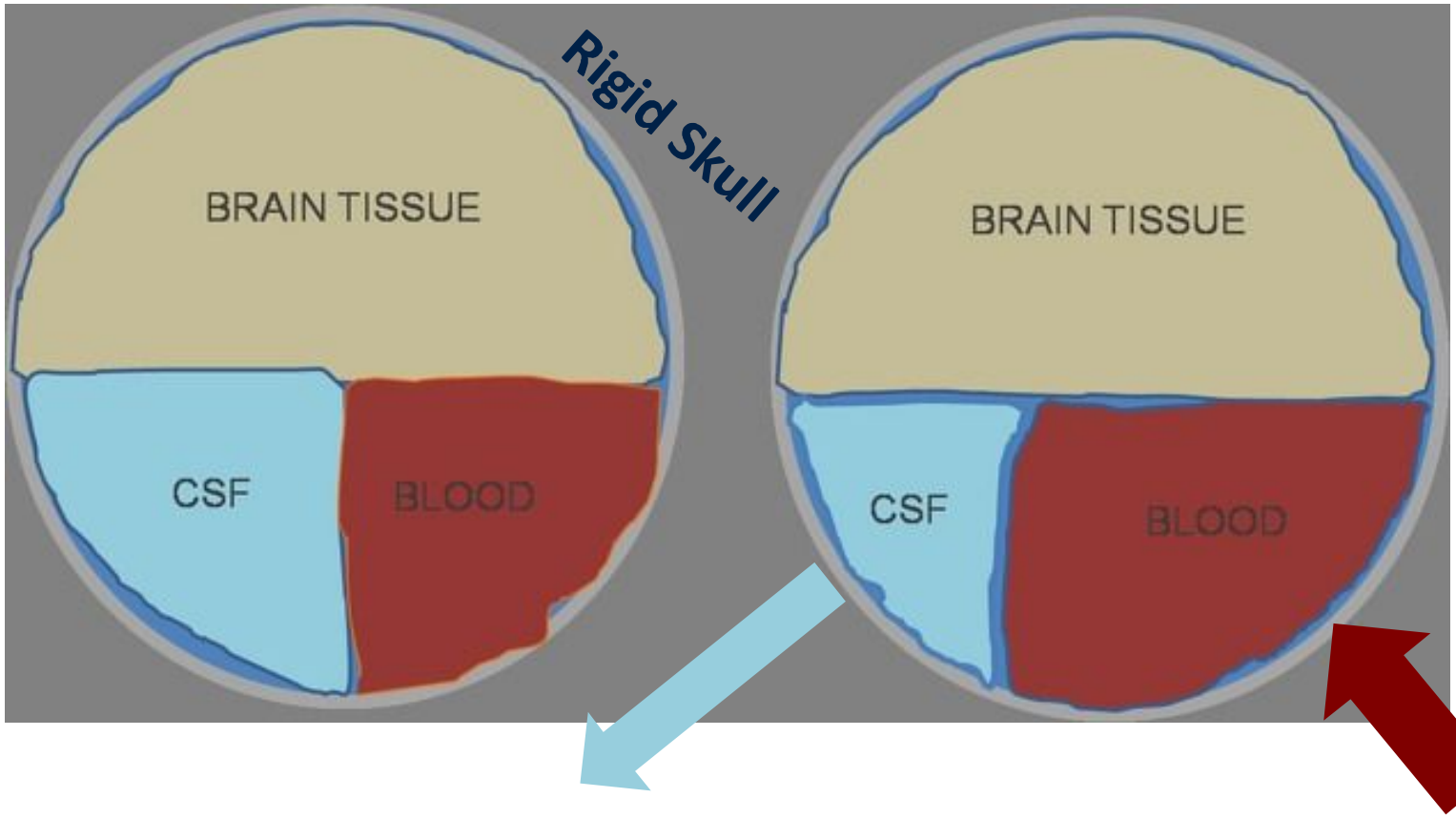

Arterial blood enters: Because of deformability of tissue, it cannot exit immediately as venous outflow, leading to an increase in CBV.

Poroelasticity

Monro-Kellie doctrine:

- Skull is rigid = cranial volume is constant
- Blood enters the brain = something has to give
- CSF is “squeezed” out as a result

Poroelasticity

Monro-Kellie doctrine:

- Skull is rigid = cranial volume is constant
- Blood enters the brain = something has to give
- CSF is “squeezed” out as a result

Poroelasticity

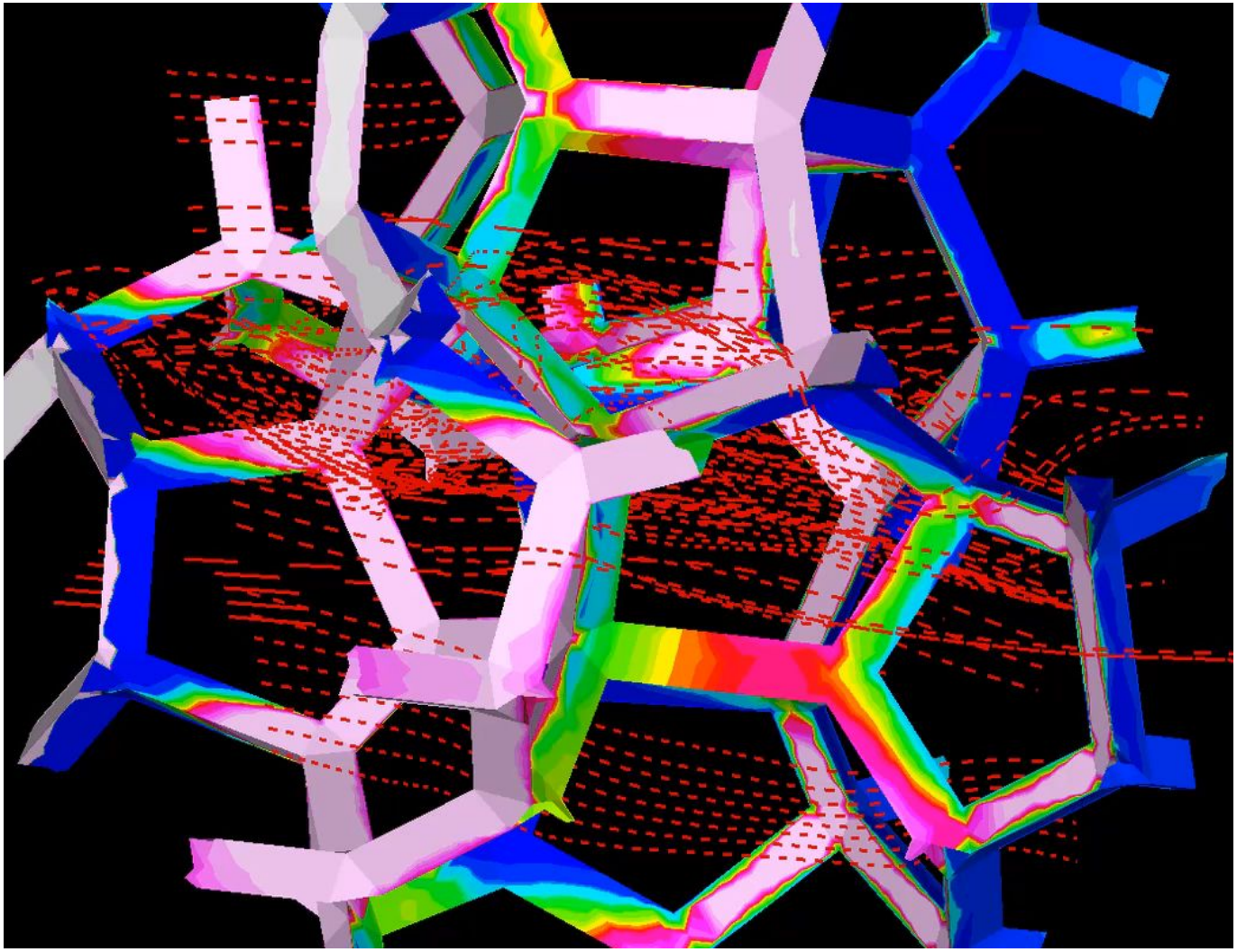

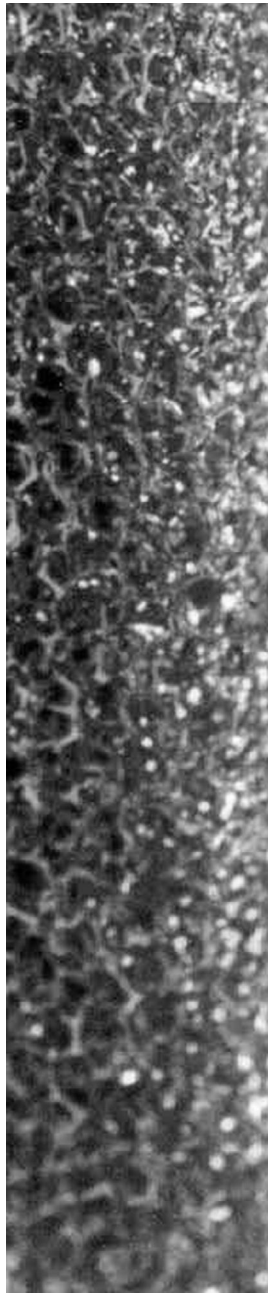

Poroelasticity

Instead of accounting for the two phases separately, we can “homogenise”: bundle a statistically adequate number or pores in a control volume and combine conservation of mass, conservation of momentum, a stress-strain relationship and a series of assumptions, the most important being that normal load is born by the fluid phase and the solid matrix together. Then:

$$E^\star \frac{\partial p}{\partial r} = \frac{\partial^2 u}{\partial r^2} + \frac{2}{r}\frac{\partial u}{\partial r} - 2\frac{u}{r^2}$$

$$\frac{\partial^2 p}{\partial r^2} = -\frac{2}{r}\frac{\partial p}{\partial r}$$

$$E^\star = \frac{\alpha(1+\nu)(1-2\nu)}{E(1-\nu)}$$

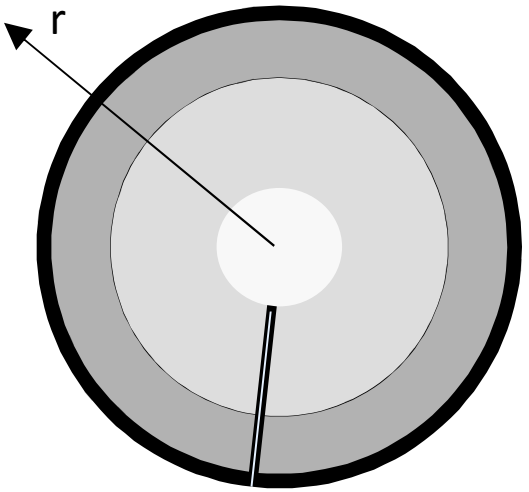

Multicompartmental Poroelasticity

- MPET has long been used in geotechnical engineering to describe fluid transport in soil and rock
  - The potential of this methodology has not been explored fully in brain biomechanics
- Deformable elastic matrix + multiple fluid networks of pores and fissures with varying porosity and permeability.
- Equations are built by treating the different fluid networks as separate compartments that are in communication.

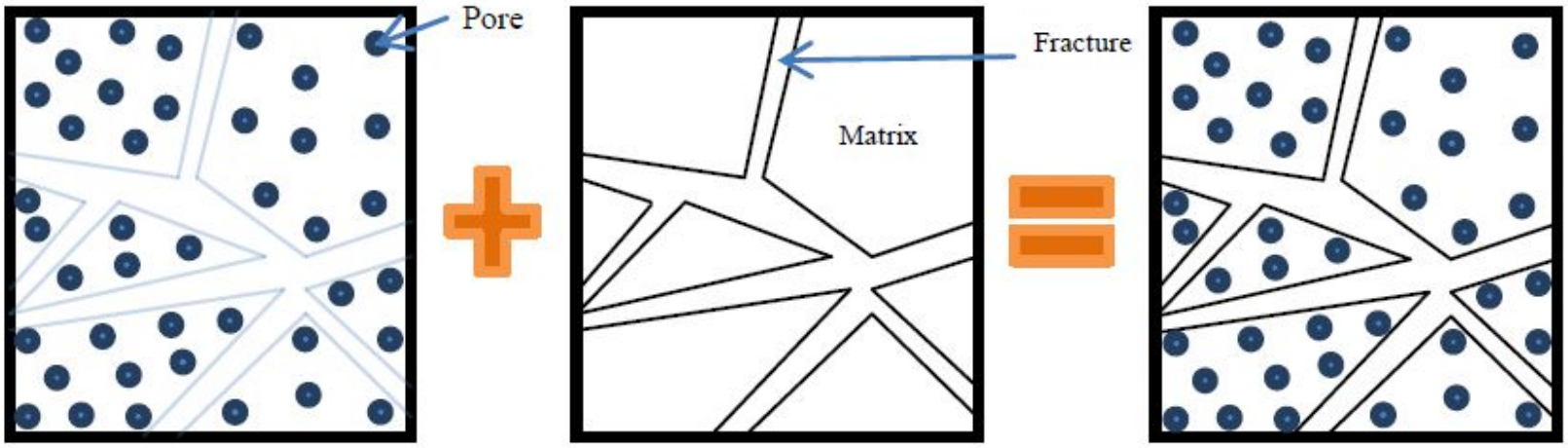

Multicompartmental Poroelasticity

- The general derivation includes the acceleration of the fluid relative to the matrix – we neglect this term for slow biological evolutions; casting in *u-p* formulation
- Solid-fluid equation of motion

$$\nabla \cdot \boldsymbol{\sigma}' - \sum_{a=1}^{A} \alpha^a \nabla p^a + \rho \left(b - \frac{\partial^2 u}{\partial t^2} \right) = 0$$

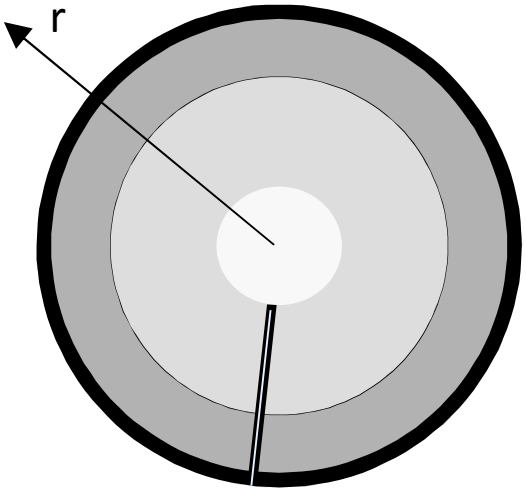

- Fluid equilibrium and conservation (each network A=1,...,a)

$$\frac{1}{Q^a} \frac{\partial p^a}{\partial t} + \alpha^a \frac{\partial (\nabla \cdot u)}{\partial t} + \nabla \cdot \left[k^a \cdot \rho^a \left(b - \frac{\partial^2 u}{\partial t^2} \right) - k^a \cdot \nabla p^a \right] - \sum_{b=1, b \neq a}^{A} \dot{s}_{b \to a} = 0$$

Multicompartmental Poroelasticity

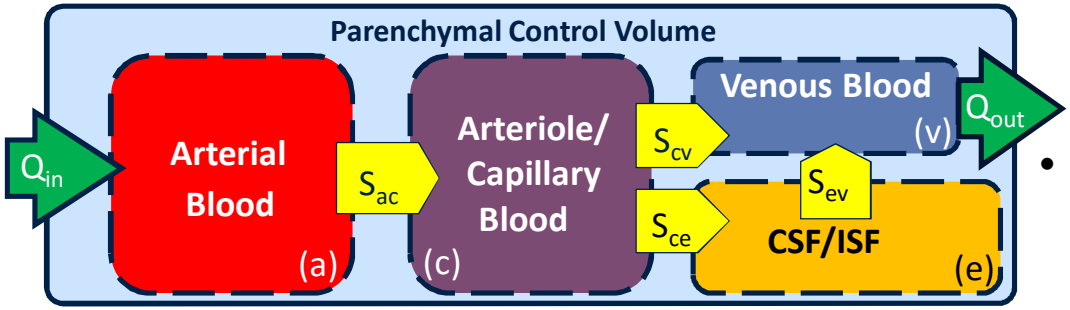

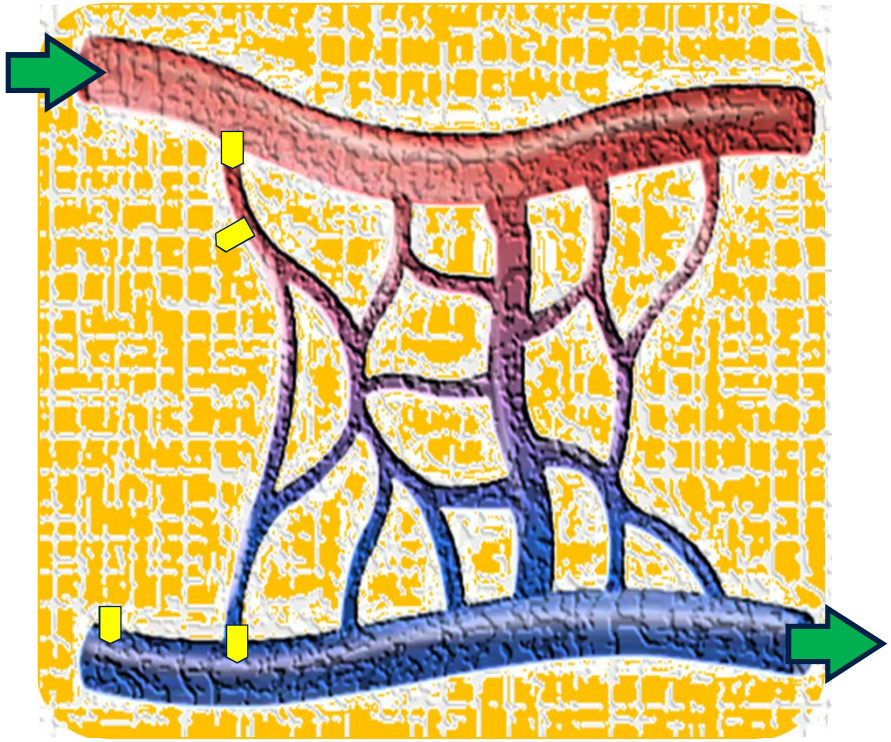

- Can capture the dynamics of *all fluids* transfer in the brain.
- The MPET framework is extended to include *independent* networks for the cerebral blood and CSF.
- Four Networks :
  1. Arterial blood,
  2. Arteriole/capillary blood
  3. CSF
  4. Venous Blood
- Flow assumptions leave ten unknowns:

α_a	α_c	α_v	
k_a	k_c	k_v	
γ_{ac}	γ_{ce}	γ_{cv}	γ_{ev}

Multicompartmental Poroelasticity

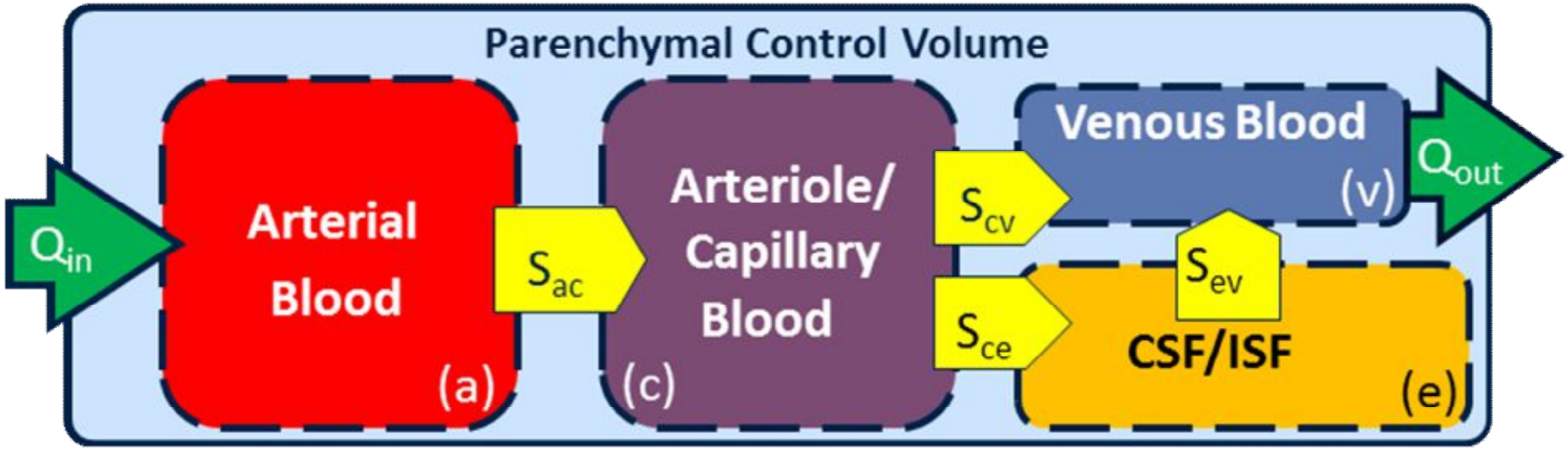

Multicompartmental Poroelasticity

Multicompartmental Poroelasticity

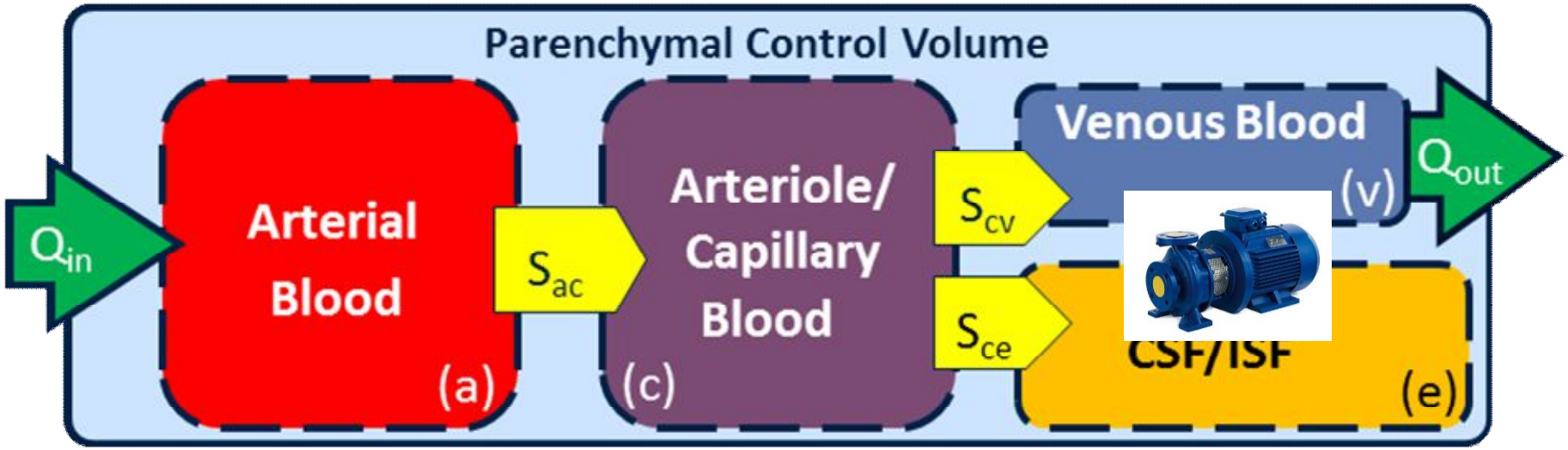

Multicompartmental Poroelasticity

- Setting *A=4* from previous slide and assuming a *linear stress-strain* relationship, we have the following *u-p* formulations:

$$G\nabla^2 \mathrm{u} + \frac{G}{1-2\nu}\nabla(\nabla\cdot\mathrm{u}) - \alpha^a\nabla p^a - \alpha^c\nabla p^c - \alpha^e\nabla p^e - \alpha^v\nabla p^v + \rho\left(\mathrm{b} - \frac{\partial^2 \mathrm{u}}{\partial t^2}\right) = 0,$$

$$\frac{1}{Q}\frac{\partial p^a}{\partial t} + \alpha^a\frac{\partial(\nabla\cdot\mathrm{u})}{\partial t} - k^a\nabla^2 p^a + k^a\nabla\cdot\left[\rho^a\left(\mathrm{b} - \frac{\partial^2 \mathrm{u}}{\partial t^2}\right)\right] - \dot{s}_{c\to a} - \dot{s}_{e\to a} - \dot{s}_{v\to a} = 0,$$

$$\frac{1}{Q}\frac{\partial p^c}{\partial t} + \alpha^c\frac{\partial(\nabla\cdot\mathrm{u})}{\partial t} - k^c\nabla^2 p^c + k^c\nabla\cdot\left[\rho^c\left(\mathrm{b} - \frac{\partial^2 \mathrm{u}}{\partial t^2}\right)\right] - \dot{s}_{a\to c} - \dot{s}_{e\to c} - \dot{s}_{v\to c} = 0,$$

$$\frac{1}{Q}\frac{\partial p^e}{\partial t} + \alpha^e\frac{\partial(\nabla\cdot\mathrm{u})}{\partial t} - k^e\nabla^2 p^e + k^e\nabla\cdot\left[\rho^e\left(\mathrm{b} - \frac{\partial^2 \mathrm{u}}{\partial t^2}\right)\right] - \dot{s}_{a\to e} - \dot{s}_{c\to e} - \dot{s}_{v\to e} = 0,$$

$$\frac{1}{Q}\frac{\partial p^v}{\partial t} + \alpha^v\frac{\partial(\nabla\cdot\mathrm{u})}{\partial t} - k^v\nabla^2 p^v + k^v\nabla\cdot\left[\rho^v\left(\mathrm{b} - \frac{\partial^2 \mathrm{u}}{\partial t^2}\right)\right] - \dot{s}_{a\to v} - \dot{s}_{c\to v} - \dot{s}_{e\to v} = 0,$$

The biological MPET model captures flow across scales and networks in soft cerebral tissue – and can be used as an embedding platform for more specific models

Multicompartmental Poroelasticity

- Setting *A=4* from previous slide and assuming a *linear stress-strain* relationship, we have the following *u-p* formulations:

$$G\nabla^2\mathrm{u}+\frac{G}{1-2\nu}\nabla(\nabla\cdot\mathrm{u})-\alpha^a\nabla p^a-\alpha^c\nabla p^c-\alpha^e\nabla p^e-\alpha^v\nabla p^v+\rho\left(\mathrm{b}-\frac{\partial^2\mathrm{u}}{\partial t^2}\right)=0,$$

$$\frac{1}{Q}\frac{\partial p^a}{\partial t}+\alpha^a\frac{\partial(\nabla\cdot\mathrm{u})}{\partial t}-k^a\nabla^2p^a+k^a\nabla\cdot\left[\rho^a\left(\mathrm{b}-\frac{\partial^2\mathrm{u}}{\partial t^2}\right)\right]-\dot{s}_{c\to a}-\dot{s}_{e\to a}-\dot{s}_{v\to a}=0,$$

$$\frac{1}{Q}\frac{\partial p^c}{\partial t}+\alpha^c\frac{\partial(\nabla\cdot\mathrm{u})}{\partial t}-k^c\nabla^2p^c+k^c\nabla\cdot\left[\rho^c\left(\mathrm{b}-\frac{\partial^2\mathrm{u}}{\partial t^2}\right)\right]-\dot{s}_{a\to c}-\dot{s}_{e\to c}-\dot{s}_{v\to c}=0,$$

$$\frac{1}{Q}\frac{\partial p^e}{\partial t}+\alpha^e\frac{\partial(\nabla\cdot\mathrm{u})}{\partial t}-k^e\nabla^2p^e+k^e\nabla\cdot\left[\rho^e\left(\mathrm{b}-\frac{\partial^2\mathrm{u}}{\partial t^2}\right)\right]-\dot{s}_{a\to e}-\dot{s}_{c\to e}-\dot{s}_{v\to e}=0,$$

$$\frac{1}{Q}\frac{\partial p^v}{\partial t}+\alpha^v\frac{\partial(\nabla\cdot\mathrm{u})}{\partial t}-k^v\nabla^2p^v+k^v\nabla\cdot\left[\rho^v\left(\mathrm{b}-\frac{\partial^2\mathrm{u}}{\partial t^2}\right)\right]-\dot{s}_{a\to v}-\dot{s}_{c\to v}-\dot{s}_{e\to v}=0,$$

The biological MPET model captures flow across scales and networks in soft cerebral tissue – and can be used as an embedding platform for more specific models

Multicompartmental Poroelasticity

- **Fluid phase**

$$\frac{1}{M_a}\frac{\partial p_a}{\partial t} + \alpha_a \frac{\partial \varepsilon}{\partial t} = \frac{k_a}{\mu_a}\nabla^2 p_a + (\hat{s}_{c\to a} + \hat{s}_{e\to a} + \hat{s}_{v\to a}) \qquad \text{arterial blood } (\boldsymbol{a})$$

$$\frac{1}{M_c}\frac{\partial p_c}{\partial t} + \alpha_c \frac{\partial \varepsilon}{\partial t} = \frac{k_c}{\mu_c}\nabla^2 p_c + (\hat{s}_{a\to c} + \hat{s}_{e\to c} + \hat{s}_{v\to c}) \qquad \text{arteriole/capillary } (\boldsymbol{c})$$

$$\frac{1}{M_e}\frac{\partial p_e}{\partial t} + \alpha_e \frac{\partial \varepsilon}{\partial t} = \frac{k_e}{\mu_e}\nabla^2 p_e + (\hat{s}_{a\to e} + \hat{s}_{c\to e} + \hat{s}_{v\to e}) \qquad \text{extracellular/CSF } (\boldsymbol{e})$$

$$\frac{1}{M_v}\frac{\partial p_v}{\partial t} + \alpha_v \frac{\partial \varepsilon}{\partial t} = \frac{k_v}{\mu_v}\nabla^2 p_v + (\hat{s}_{a\to v} + \hat{s}_{c\to v} + \hat{s}_{e\to v}) \qquad \text{venous blood } (\boldsymbol{v})$$

- **Solid phase**

$$G\nabla^2 u + (G+\lambda)\frac{\partial \varepsilon}{\partial x} = \frac{\partial}{\partial x}(\alpha_a p_a + \alpha_c p_c + \alpha_e p_e + \alpha_v p_v) - F_x$$

$$G\nabla^2 v + (G+\lambda)\frac{\partial \varepsilon}{\partial y} = \frac{\partial}{\partial y}(\alpha_a p_a + \alpha_c p_c + \alpha_e p_e + \alpha_v p_v) - F_y$$

$$G\nabla^2 w + (G+\lambda)\frac{\partial \varepsilon}{\partial z} = \frac{\partial}{\partial z}(\alpha_a p_a + \alpha_c p_c + \alpha_e p_e + \alpha_v p_v) - F_z$$

New findings – extending MPET

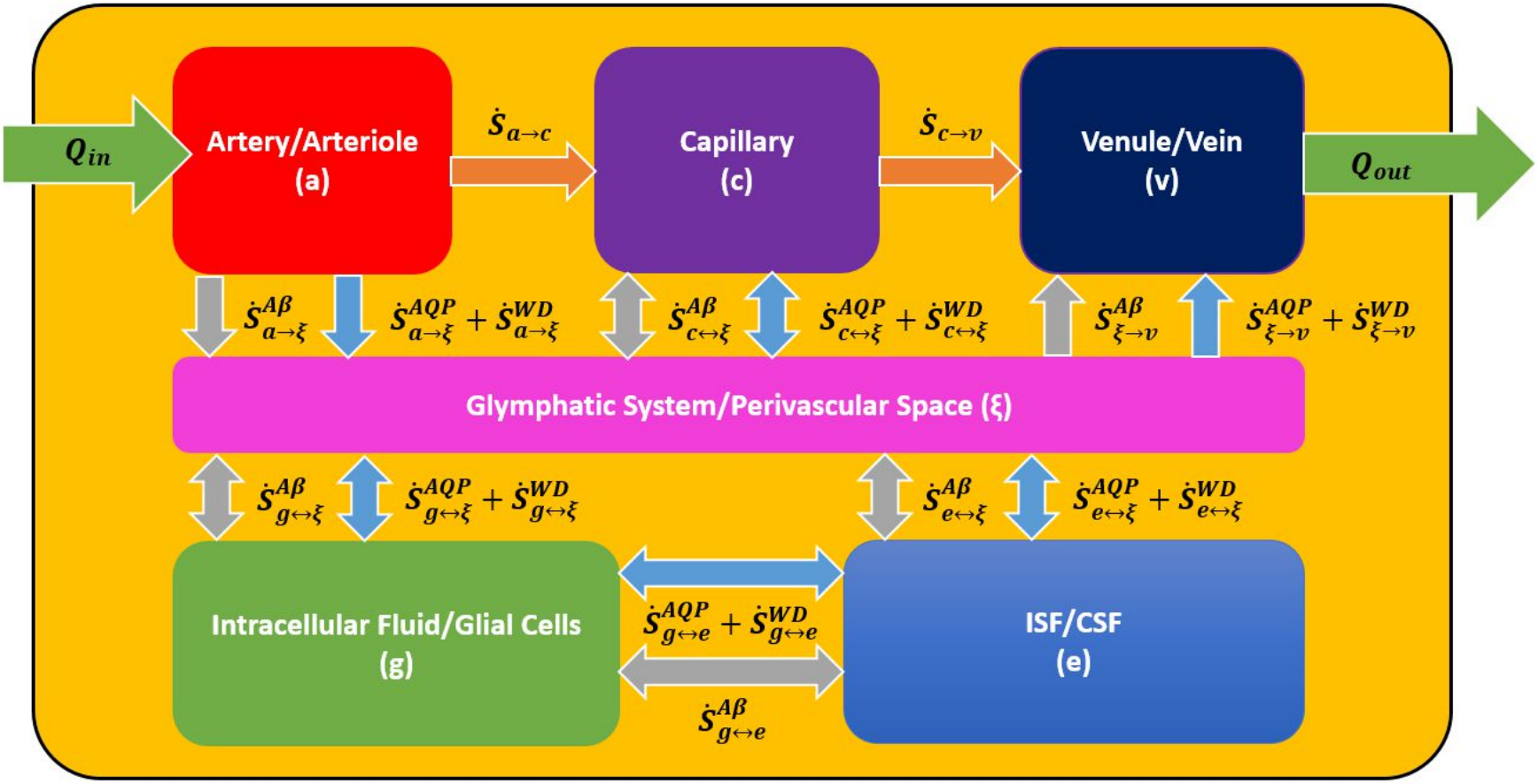

FEM u-p formulations

$$\mathbf{u} = \begin{bmatrix} u \\ v \\ w \end{bmatrix} = \begin{bmatrix} \sum_{i=1}^{n_n} N_i u_i \\ \sum_{i=1}^{n_n} N_i v_i \\ \sum_{i=1}^{n_n} N_i w_i \end{bmatrix}$$

$$p_i = \sum_{j=1}^{n_n} N_j p_j \quad (i = a, c, e, v)$$

$$\mathbf{K}\mathbf{u} - (\mathbf{Q}_a\mathbf{p}_a + \mathbf{Q}_c\mathbf{p}_c + \mathbf{Q}_e\mathbf{p}_e + \mathbf{Q}_v\mathbf{p}_v) = \mathbf{F}$$

$$\mathbf{A}\dot{p} + \mathbf{B}p = \mathbf{P}$$

$$\mathbf{K} = \int_\Omega \mathbf{B}^T\mathbf{D}\mathbf{B}d\Omega$$

$$\mathbf{A} = \int_\Omega \frac{1}{M_i}\mathbf{N}\mathbf{N}^T d\Omega$$

$$\mathbf{Q}_i = \int_\Omega \alpha_i \mathbf{B}^T \mathbf{h} d\Omega$$

$$\mathbf{B} = \int_\Omega \frac{k_i}{\mu_i}\nabla\mathbf{N}\nabla\mathbf{N}^T d\Omega$$

$$\mathbf{F} = \int_\Omega N^T \mathbf{b} d\Omega + \int_{\Gamma_N} N^T \mathbf{t}_N d\Gamma$$

$$\mathbf{P} = \int_\Omega \hat{s}\mathbf{N}d\Omega - \int_\Omega \alpha_i \dot{\epsilon}\mathbf{N}d\Omega$$

Embedding MPET in the VPH-DARE@IT Personalised Workflow

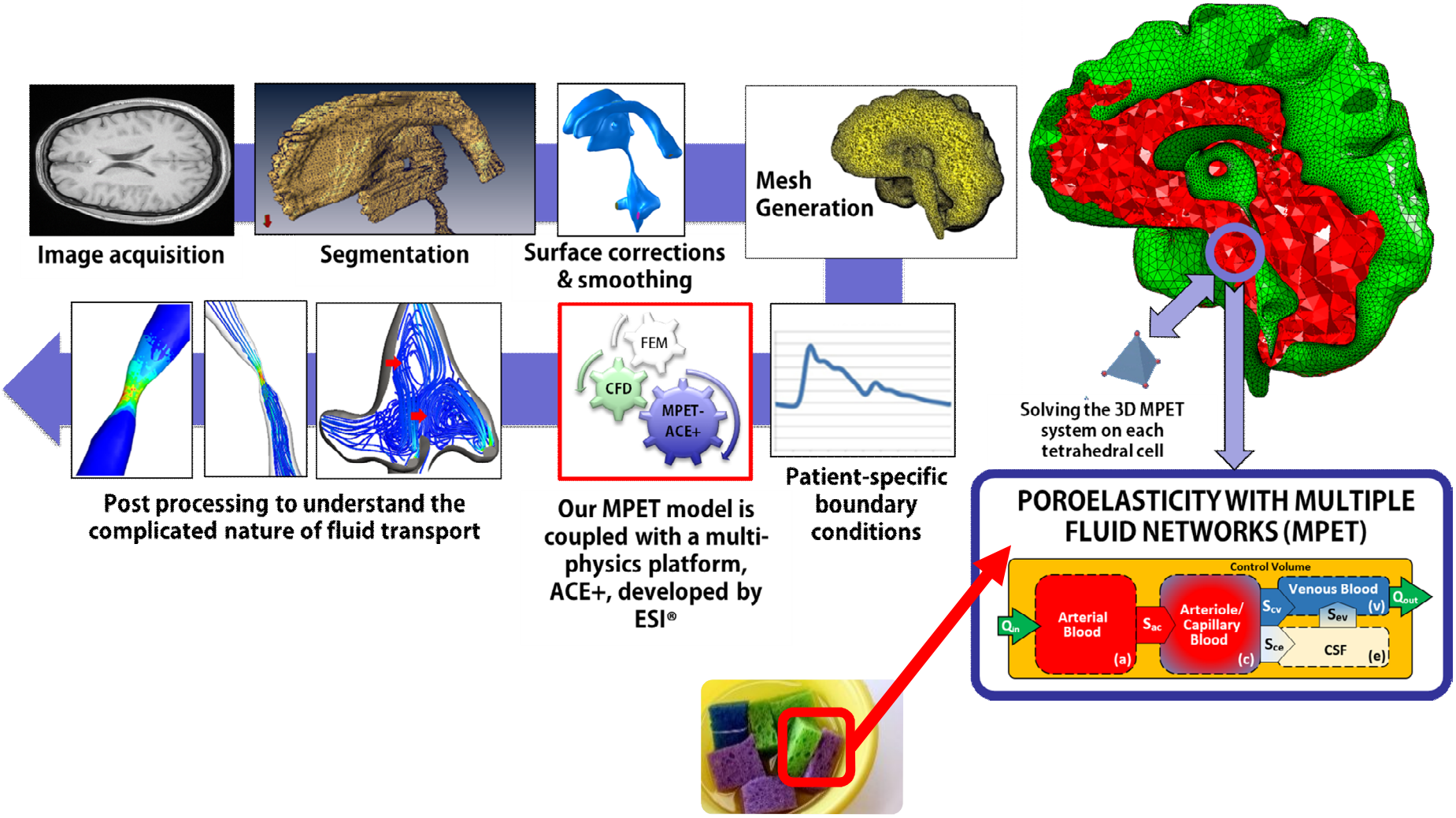

Results: Image Processing, Segmentation and Surface/Volume Reconstruction

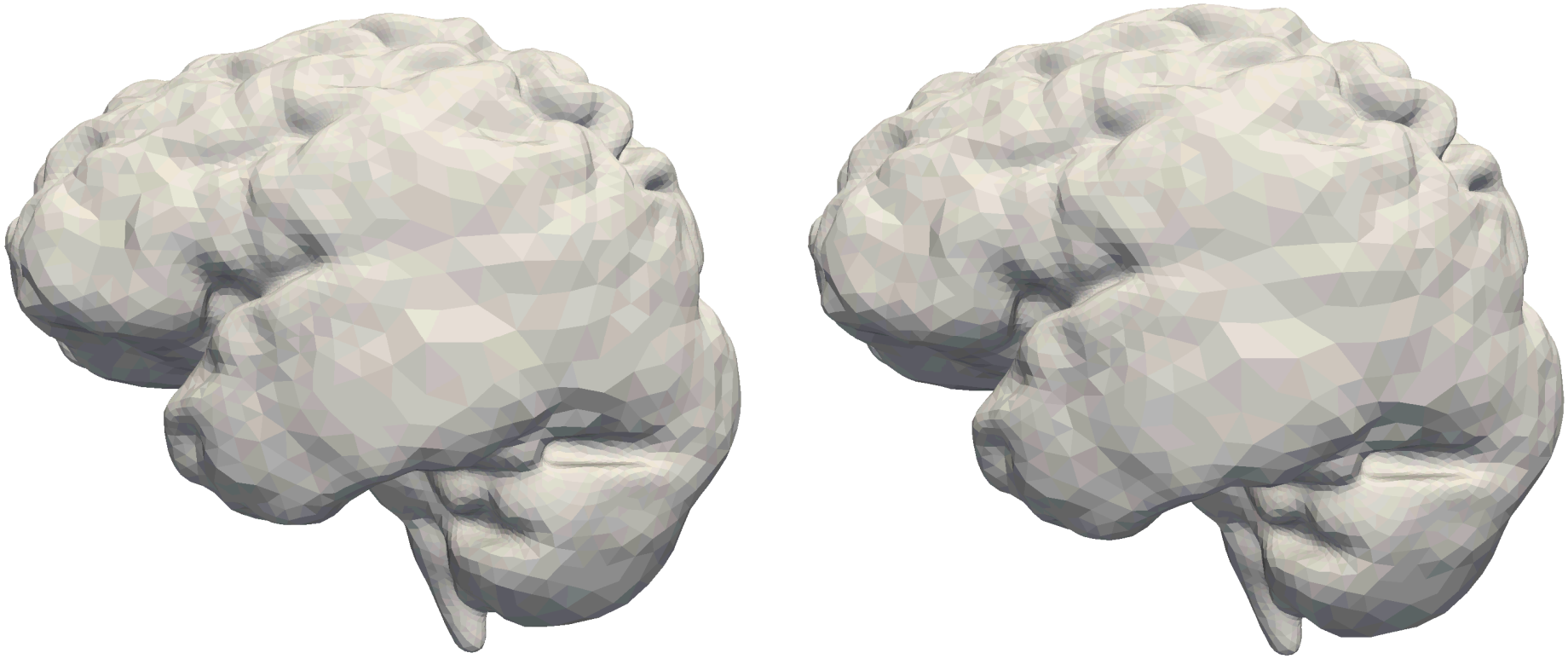

Results: Features identification

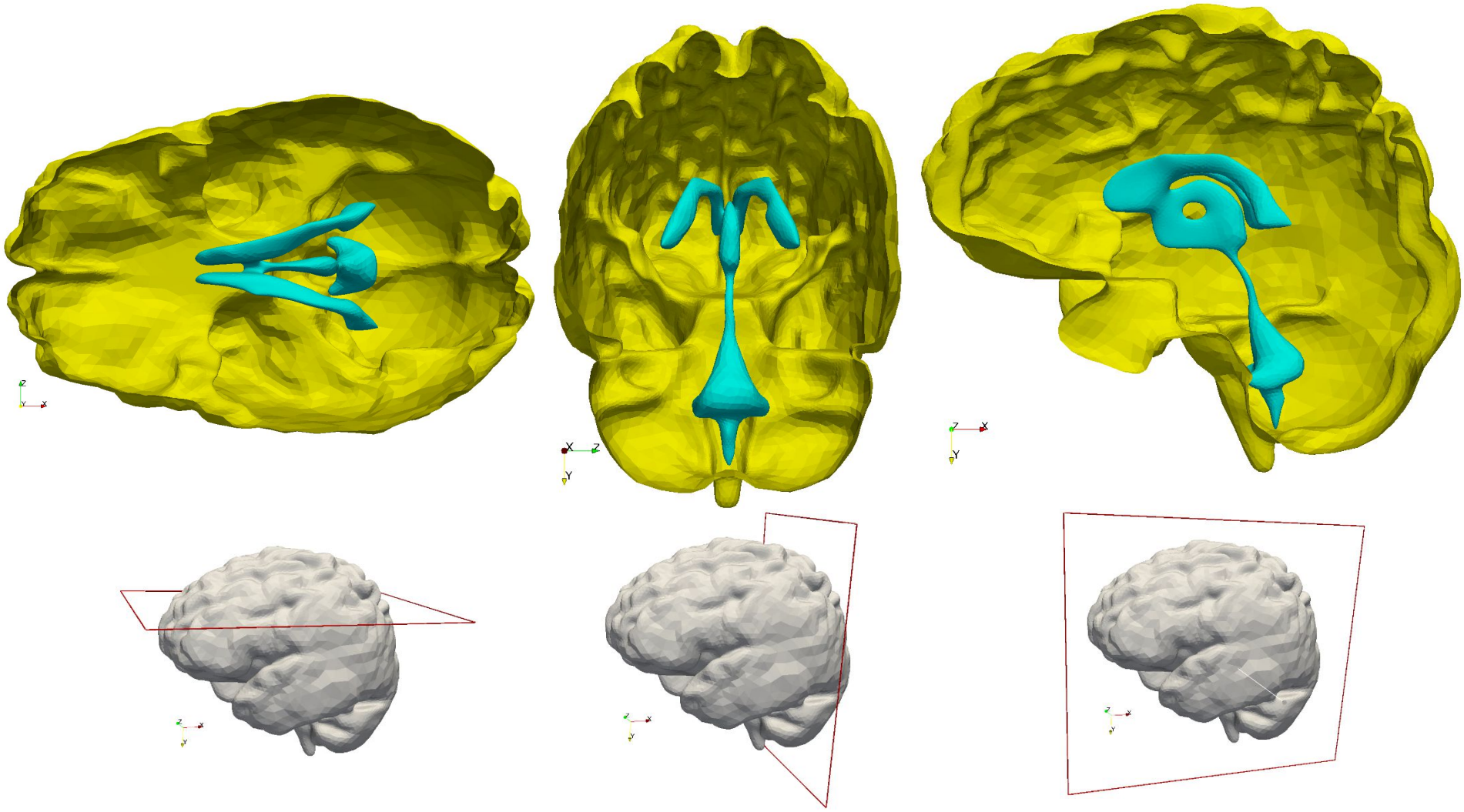

Results: Mesh Generation

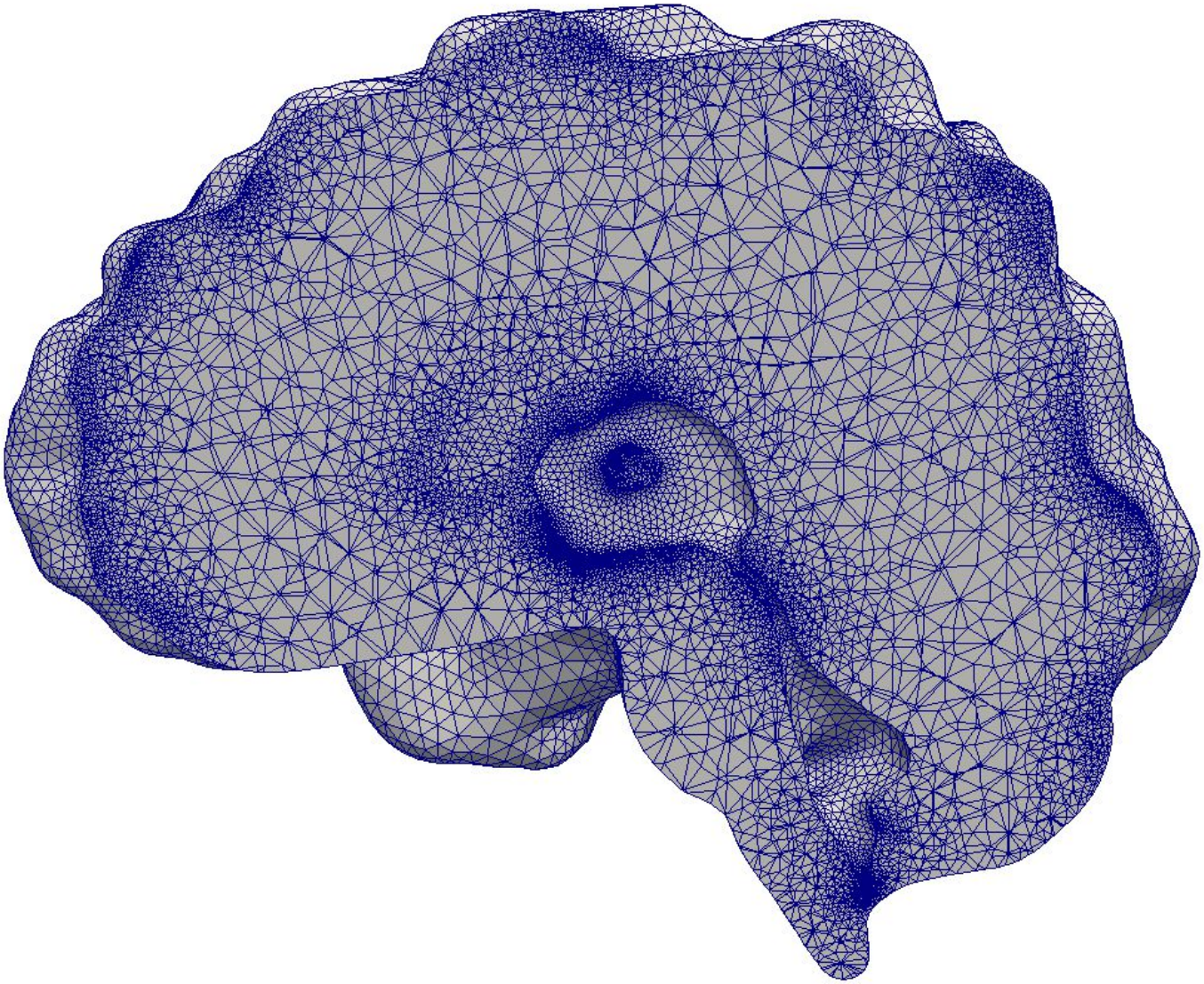

Results: Quantities of Interest

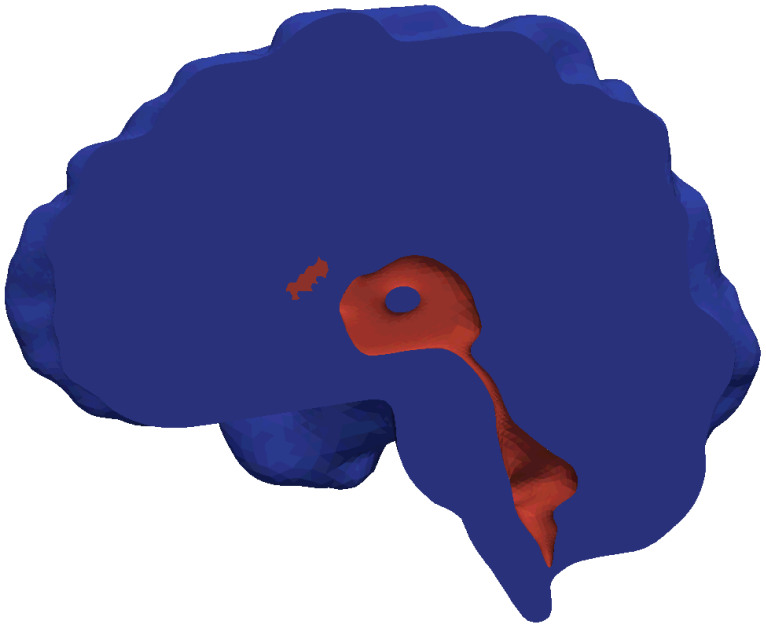

CSF pressure

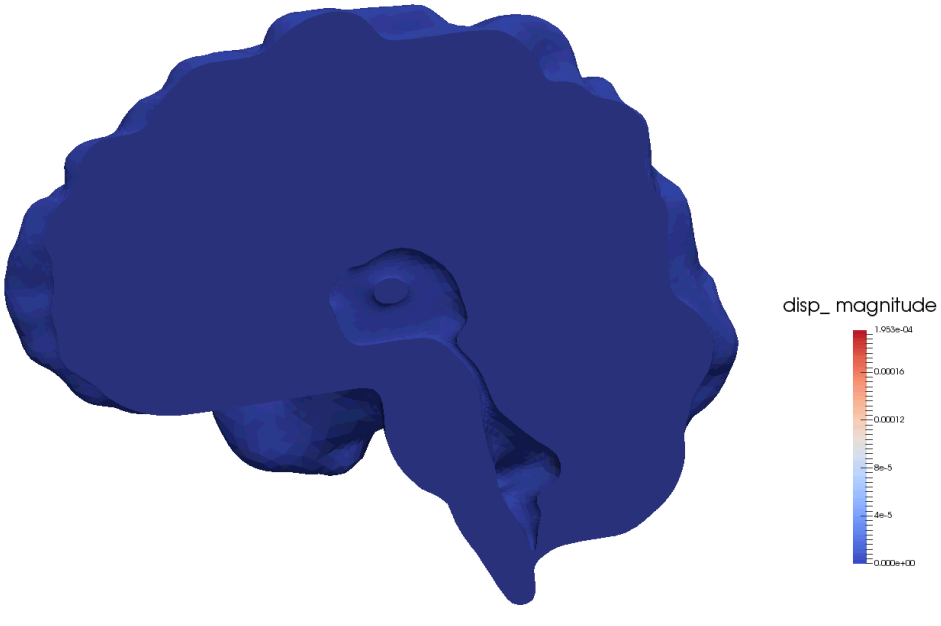

Displacement magnitude

Results: Ventricular Hydrodynamics

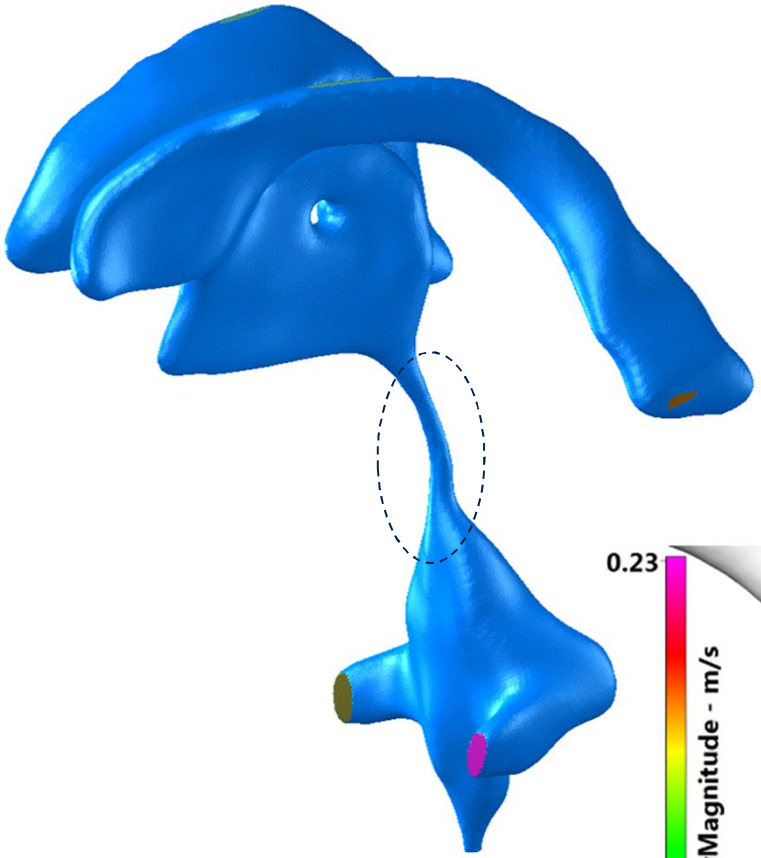

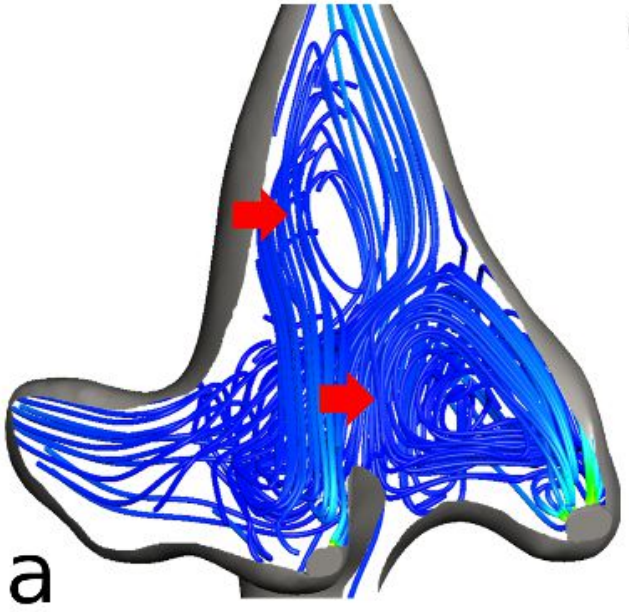

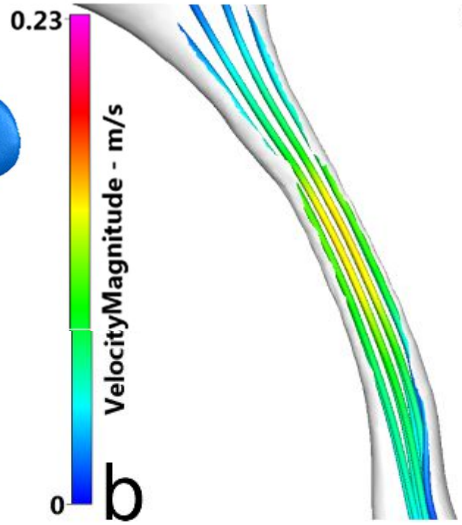

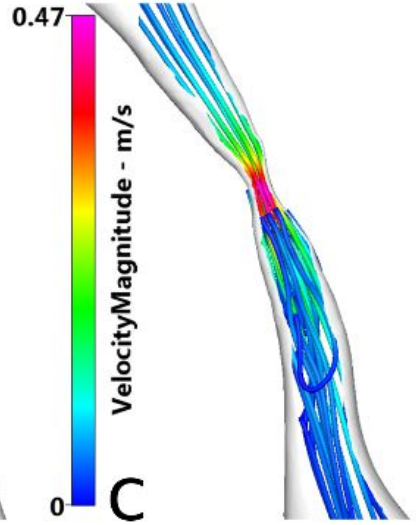

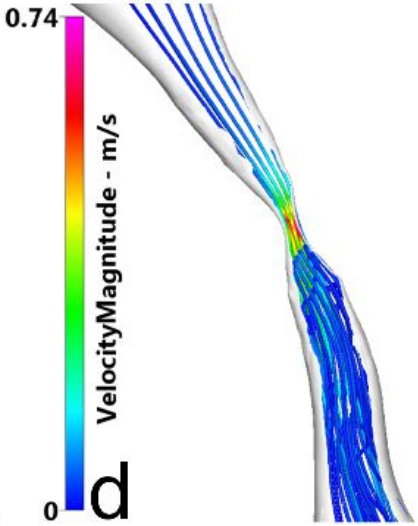

1D Results (compact FD) *nD-nD coupling*

Aqueductal stenosis and ETV

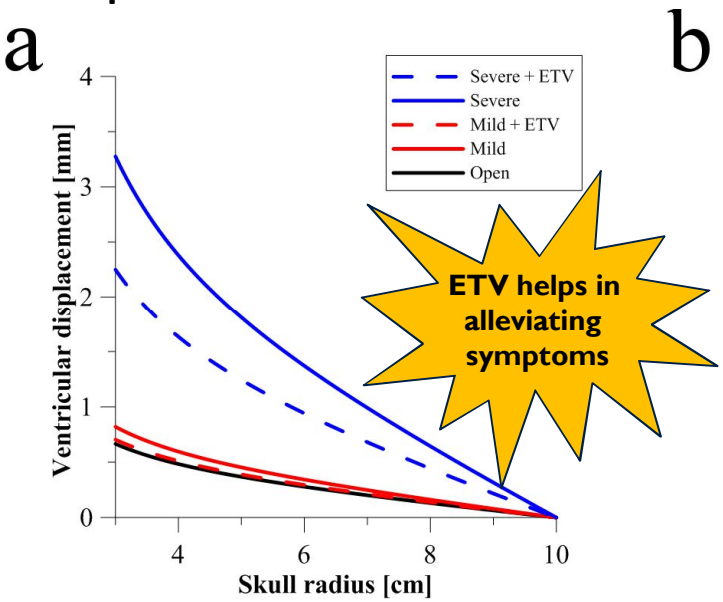

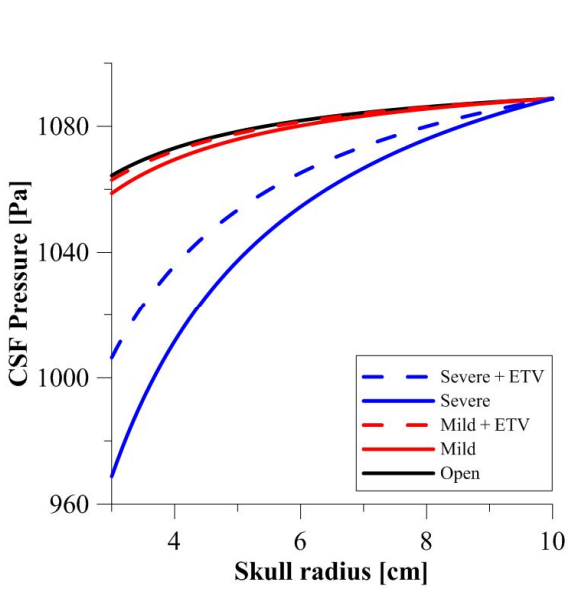

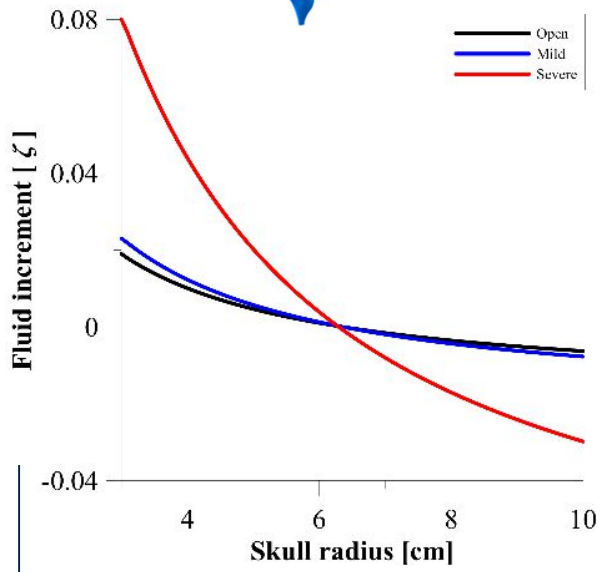

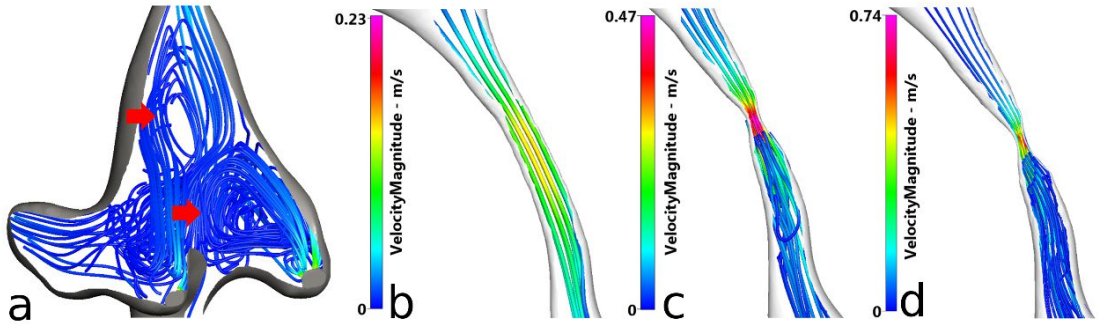

$$\zeta_e = a^e \varepsilon + \frac{\alpha^e \left(1 - \alpha^e \beta^e\right)}{K \beta^e} p_e$$

1. Vardakis JC, Tully BJ, Ventikos Y (2013) Exploring the Efficacy of Endoscopic Ventriculostomy for Hydrocephalus Treatment via a Multicompartmental Poroelastic Model of CSF Transport: A Computational Perspective. **PLoS ONE** 8(12): e84577. doi:10.1371/journal.pone.0084577

2. Vardakis JC, Tully BJ, Ventikos Y (2013) Multicompartmental poroelasticity as a platform for the integrative modelling of water transport in the brain. In: Holzapfel GA, Kuhl E, editors. **Computer Models in Biomechanics: from Nano to Macro**. Heidelberg: Springer-Verlag. 305–316.

Results: H_2O content, clearance & perfusion

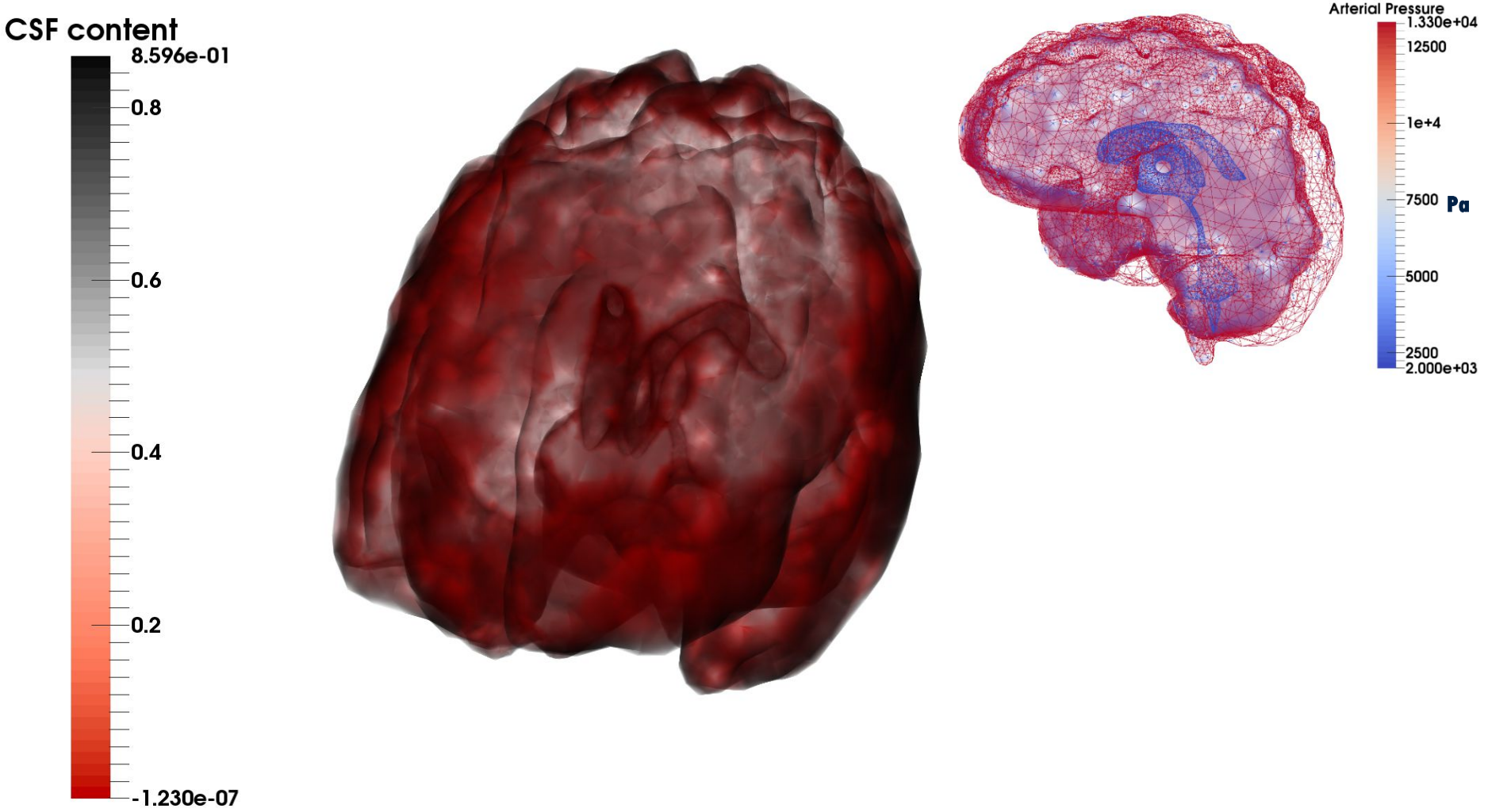

Results: Compartmental pressures & flows

CSF/ISF fluid increment

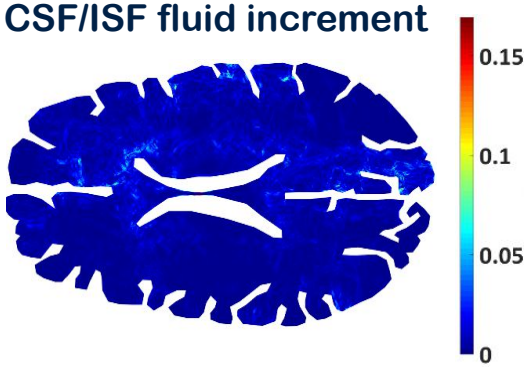

Darcy velocity of capillary compartment [m/s]

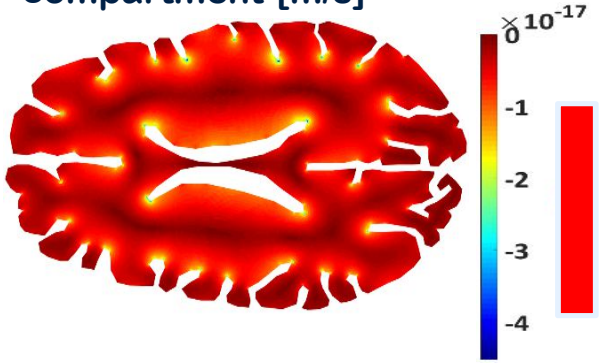

CSF/ISF pore pressure

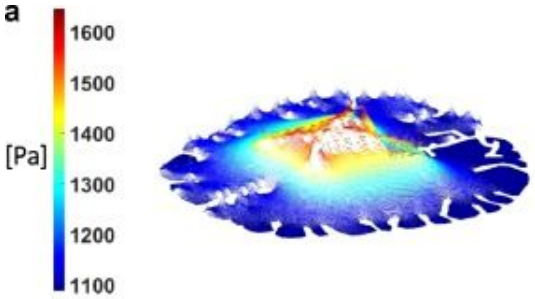

Venous pore pressure

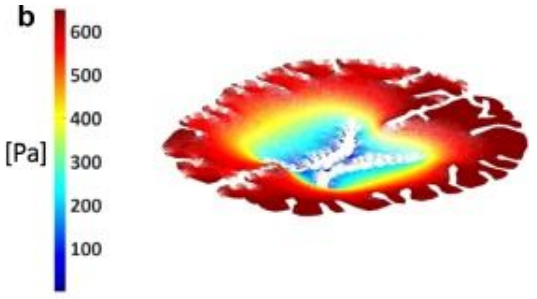

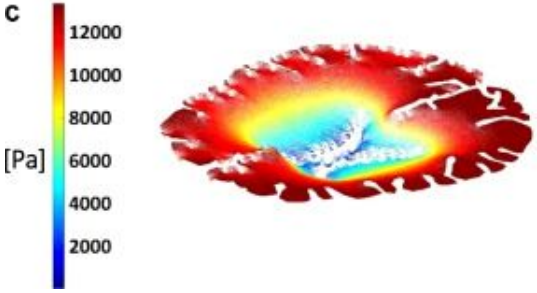

Arterial pore pressure

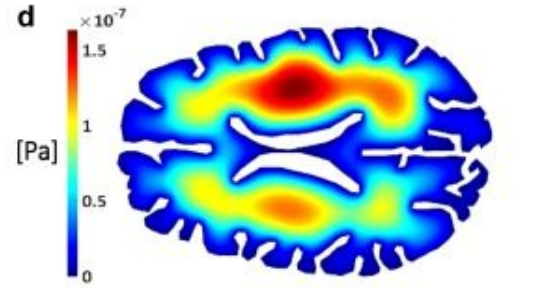

Capillary pore pressure

Results: Transient Intracranial Pressure (ICP) profiles

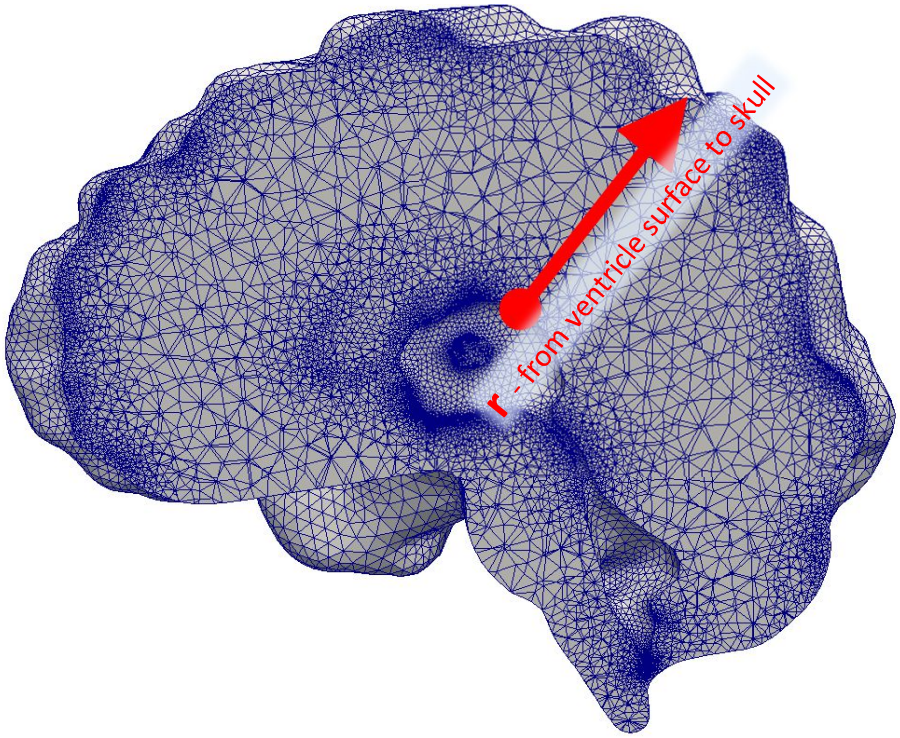

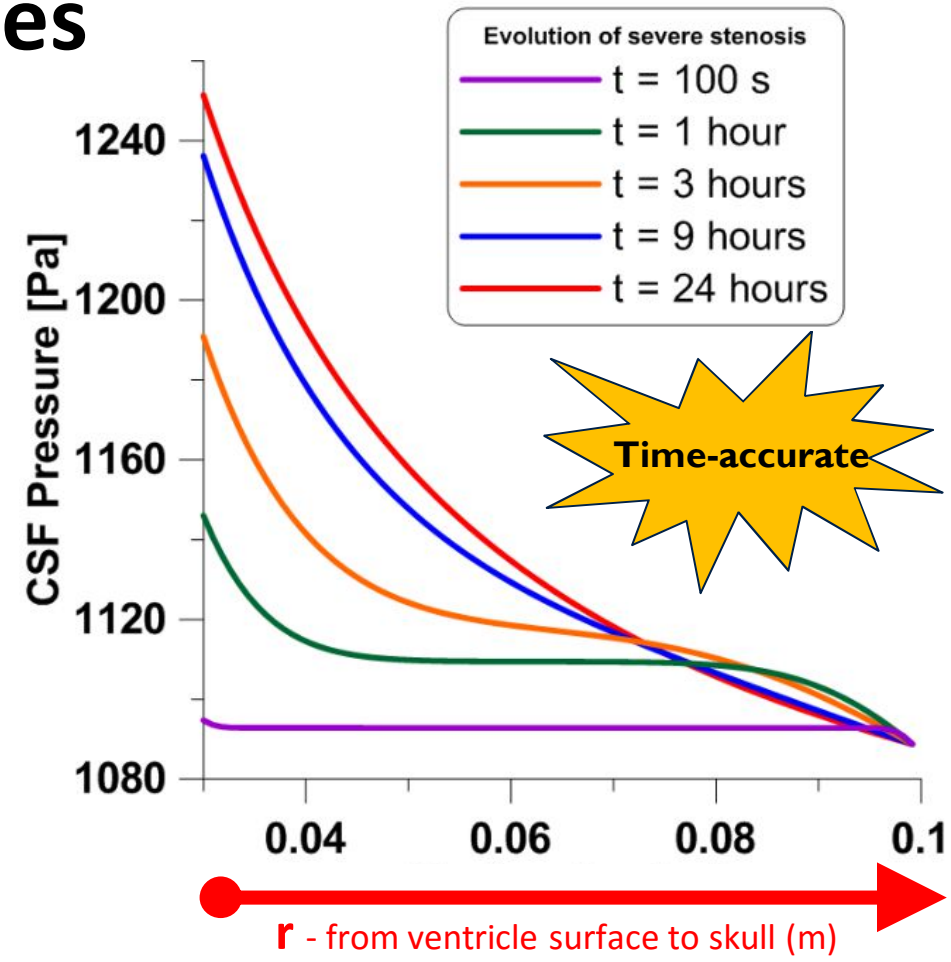

NPH

•Multicompartmental Poroelasticity allowed us to explore this intricate hypothesis:

- ➢A congenital condition involving the **stiffness of the arterioles** leads to **small (sub-cm) ventricular distension** – extremely difficult to observe clinically.
- ➢A condition, in later life, involving **increased leakiness** from the capillaries to the extracellular environment, leads to **no measurable ventricular distension.**

•The model reveals that the **combination of the two conditions** described above produces **ventricular displacements of 4cm**, exactly the range observed in NPH, with a **completely unobstructed aqueduct!**

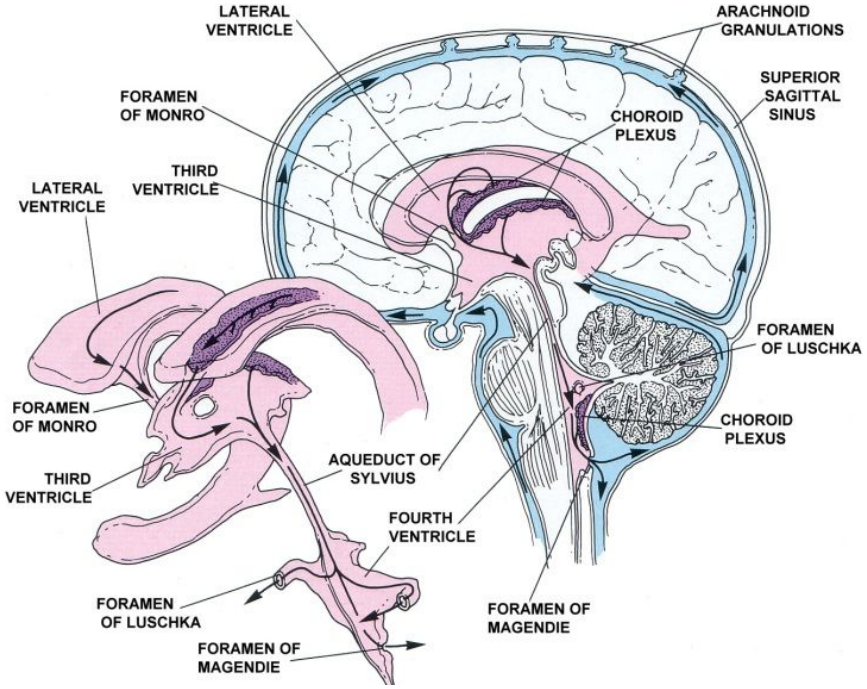

NPH

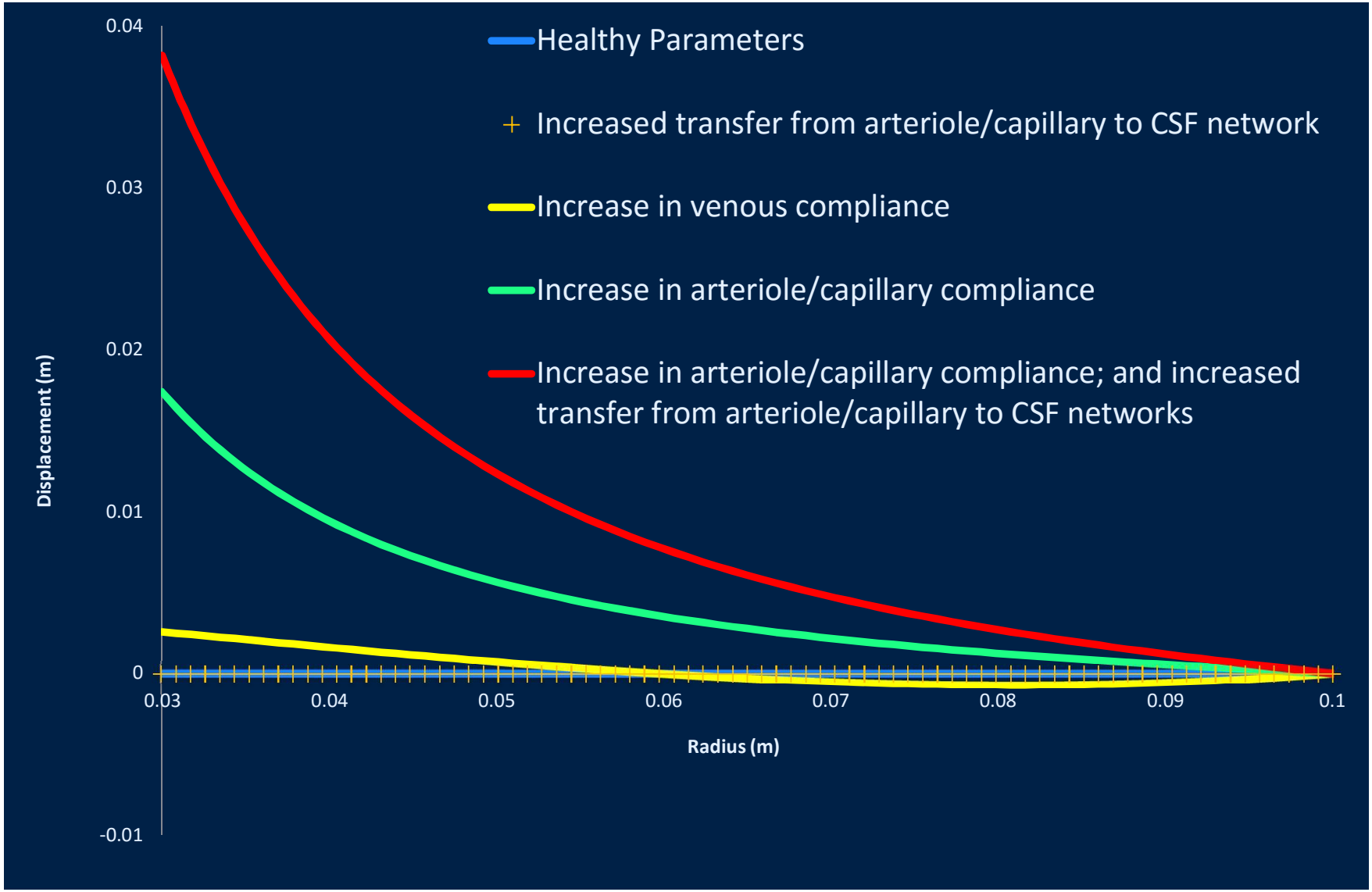
Healthy Parameters
Increased transfer from arteriole/capillary to CSF network
Increase in venous compliance
Increase in arteriole/capillary compliance
Increase in arteriole/capillary compliance; and increased transfer from arteriole/capillary to CSF networks
Displacement (m)
0.04
0.03
0.02
0.01
0
-0.01
0.03
0.04
0.05
0.06
0.07
0.08
0.09
0.1
Radius (m)

Conclusions

- MPET is a naturally mutiscalar environment for modelling perfused deformable tissue.

- Capable of processing patient-specific brain imaging data and of further personalisation with the application of patient-derived hemodynamic conditions.

- Validation so far: can capture ventricular dilatation and ICP from “first principles” – further validation needed regarding perfusion and clearance maps.

Work in progress

- Personalisation & properties (MRE, DTMR)
- 6-MPET – pursue vigorously regarding constants and parameters (perivascular/glymphatic & astrocytic compartments)
- Osmosis & ions
- Better “solid matrix” constitutive laws (work in Zurich?)
- Brain tissue remodelling:
  - Vascular, ok-ish
  - Demyelination?
  - ???

Acknowledgements

For immensely hard work:

- Dr Brett Tully
- Dr John Vardakis
- Dean Chou
- Dr Liwei Guo

For particularly enlightening discussions:

- Prof Ole Petter Ottersen (Oslo)
- Prof Stig Omholt (Oslo)
- Prof Erlend Nagelhus (Oslo)
- Dr Klas Pettersen (Oslo)

For most valuable interaction:

- Dr Mustafa Megahed (ESI)
- Dr Joerg Willems (ESI)

For support:

- Clarendon Fund
- CDT in Healthcare Innovation
- EPSRC
- VPHDARE@IT (EU Fr VII)

European Commission
SEVENTH FRAMEWORK PROGRAMME
VPH-DARE@IT
Virtual Physiological Human: DementiA Research Enabled by IT